Intermittent production of electricity-based synthetic jet fuel as a demand-side management strategy for grid decarbonization

Glenda Chen [a], Oleg Lugovoy [b], Pedro Piris-Cabezas [c], Anna Stratton [d]

[a] Environmental Defense Fund, Raleigh, NC, USA
[b] Independent researcher and consultant, USA
[c] Environmental Defense Fund, Madrid, Spain (corresponding author, mail to: ppiris@edf.org)
[d] ClimateWorks Foundation, Madrid, Spain (while currently affiliated with ClimateWorks Foundation, her contribution to this article is from her time working for Environmental Defense Fund)

Highlights

- E-fuel pathways can unlock significant cost savings in the near- to mid-term and become cost competitive with other alternative fuels if they are designed to provide grid balancing services.
- There will be sufficient high-quality surplus renewable electricity to meet most or all of U.S. jet fuel demand in 2050, and potentially a significant fraction of demand in 2030.
- By drawing upon abundant wind power and industrial fermentation waste CO_2, e-SAF synthesized in the Midwest alone could inexpensively deliver a bulk of the 3-billion-gallon target for 2030 under the national SAF Grand Challenge.
- The grid receives substantial benefits in terms of expediting the power sector's energy transition.
- The adoption of e-fuel technology serves not only aviation, but also other hard-to-decarbonize sectors with vested interests in the co-produced long-chain synthetic hydrocarbons.
- Fully capitalizing on synergies across sectors and within the e-fuel production pathway itself is of paramount importance.

Abstract

Variable renewable energy (VRE) is poised to become a cornerstone in the effort to meet economy-wide climate change mitigation targets. However, while transport electrification is advancing for road vehicles, it remains challenging for long-haul aviation. In this hard-to-abate sector, policy and research focus on producing drop-in fuels compatible with existing aircraft technology. Although the alternative jet fuel market is currently dominated by biofuels, diversifying fuel production pathways is crucial for a resilient future. Emerging electricity-based synthetic jet fuels offer promising new routes nearing commercialization. Despite adoption barriers posed by the cost ratio between electrolytic sustainable aviation fuel (e-SAF) and conventional fossil jet fuels, techno-economic assessments involving an integrated power systems perspective suggest potential synergies to both bring down e-SAF production costs and facilitate the energy transition of the power sector towards renewables-based power generation systems. Large VRE capacity necessitates flexible demand management, with interruptible technologies like e-fuel electrolyzers potentially playing a critical role in grid balancing and cost

reduction. This analysis examines the feasibility of national-scale e-SAF deployment in the United States, considering the synergistic impacts on cost competitiveness and grid efficiency, and presents a comprehensive cost evaluation of key steps in the e-SAF production pathway, including CO_2 procurement, electrolysis, CO_2 activation, and fuel synthesis. Results indicate that e-SAF pathways designed for flexible operation can significantly reduce grid transition costs and potentially achieve cost competitiveness with biofuels. The findings underscore the feasibility and necessity of e-SAF adoption to meet aviation's global net-zero goals, emphasizing the importance of cross-sector synergies in addressing the decarbonization challenge.

Keywords

electrofuels; power to liquids; sustainable aviation fuels; green hydrogen; renewable energy; direct air capture; waste CO_2

---

1. Introduction

Variable renewable energy (VRE) will play a central role in decarbonizing electric power generation worldwide and reaching climate change mitigation targets. Yet, the transition to VRE faces substantial infrastructure investment risk, among other barriers, due to its natural variability. Furthermore, transport electrification is progressing for road vehicles but is not accessible for long-haul aviation and marine transport. In these hard-to-abate sectors, policy and research concentrate on options for producing drop-in fuels compatible with existing combustion engines.

Though the alternative jet fuel market is currently dominated by the hydroprocessed esters and fatty acids (HEFA-SPK) pathways, diversifying the suite of fuel production avenues will be critical for a versatile, resilient value web. Furthermore, it is imperative to prioritize the subset of alternative jet fuels that are truly sustainable, per rigorous international criteria defining sustainable aviation fuel (SAF). There are several relatively new methods of electricity-based synthetic jet fuel (e-SAF) production that are commercial or on the verge of commercialization and have been certified by ASTM International as safe for use in existing aircrafts (Piris-Cabezas, 2022). The cost ratio between e-SAF and conventional fossil jet is often cited as a barrier to adoption but is not set in stone; planning for the future entails projecting future techno-economics considered from an integrated power systems perspective. Grid decarbonization and expansion are already, and will continue to, undergo a massive transition that also profoundly shifts the boundary conditions for e-SAF adoption.

Once large VRE capacity is in place, the ability to manage the load becomes a critical feature for balancing the grid. In this context, a significant fraction of demand would need to be flexible, and interruptible technologies such as electrolyzers used for e-fuel or power-to-liquid (PtL) production could play a key role, potentially delivering cost benefits to both the power sector and fuel manufacturing sector.

Under the International Energy Agency (IEA)'s Net Zero by 2050 pathway scenario, electricity generation would need to reach net-zero emissions globally by 2040, which entails a dramatic overhaul of power system flexibility to ensure reliable synchronization between supply and demand. IEA

estimates that system flexibility must quadruple globally to make this scenario a reality, in tandem with a more than two-and-a-half-fold increase in electricity supply. A key source of demand flexibility would come from electrolysis-based and derivative technologies such as PtL (IEA, 2021a).

e-SAF is anticipated to be a key enabling technology for the eventual decarbonization of aviation. This pathway involves the production of an electricity intensive syngas –a mixture of hydrogen (H_2) and carbon monoxide (CO)— that is then converted into kerosene and other sizes of hydrocarbon liquids and gases by a Fischer-Tropsch (FT) reaction. The carbon used in e-SAF could ideally come from two main sustainable sources: (1) waste CO_2 from, e.g., landfill-based biogas production or cellulosic ethanol fermentation, and eventually (2) direct air capture (DAC). The latter is expected to take a growing role over time in the production of e-SAF as production costs decrease and waste CO_2 becomes scarce in a carbon-constrained world. Renewable electricity availability is the primary limiting factor setting the threshold for sustainable PtL production.

Electrolytic hydrogen-based fuels are one of the few reliable options for high-integrity SAF that can sustainably scale up to fulfil the goals set by United Nation's International Civil Aviation Organization (ICAO), governments, and businesses. Replacing 100% of international aviation fuel demand with high-integrity SAF including PtL could achieve 10 $GtCO_2$ of emissions reductions through 2050, equivalent to 65% of total forecasted CO_2 emissions from international aviation – assuming e-SAF with near-zero life-cycle emissions are deployed at scale (Piris-Cabezas, 2022). These emissions savings could increase to 17 $GtCO_2$ with domestic flights' fuel demand.

Predicting the costs of e-SAFs involves substantial modeling uncertainty because the market for both standalone DAC and e-SAF production has yet to reach scale. While each stage of the e-SAF production chain has been demonstrated, and pilot plants have come online, no facilities are yet producing e-SAF in large volumes. Therefore, to estimate e-SAF costs, we present in this paper a comprehensive cost evaluation of the key steps on the production pathway, namely: CO_2 procurement (both from waste sources and DAC), electrolysis, CO_2 activation, and fuel synthesis. Key cost variables include capital expenditures (capex) for acquiring and building facilities and plants, as well as operational expenditures (opex) such as the cost for the energy needed for DAC and electrolysis.

Literature cost estimates for the pathway given today's conditions range between four to eight times the fossil benchmark price, or roughly $2800 to 5500 per tonne of fuel (Malins, 2017; World Economic Forum [WEF], 2020; Grahn et al., 2022). However, prices are expected to rapidly decline as renewable electricity costs fall and electrolyzer and DAC technologies scale. Costs for e-SAFs are expected to be in the lower $2000s/tonne by 2030 and as low as $1000-1500 per tonne by 2050 (WEF, 2020; Schmidt et al., 2016). The more ambitious estimates – some around $1000/tonne in the near term - take VRE and flexible load as a crucial assumption in their envisioned production setups (Terwel & Kerkhoven, 2018; Millinger et al., 2021; Seymour et al., 2024), but in a different configuration than that explored in our paper, which focuses on the synergies with the power sector energy transition as a cost abatement strategy.

The cost of renewable electricity generation is one of the top two key drivers for the total cost of the e-SAF pathway, as both DAC and electrolysis are energy intensive (Fasihi et al., 2016; Grahn et al., 2022;

Malins, 2017; Dieterich et al, 2020). As such, a perspective bridging both the power and transport sectors can prove useful for tracking price dynamics.

From a grid perspective, the hourly variability of renewables presents a large-scale spatial and temporal planning challenge given that real-time demand is relatively static in current power sector configurations. When generation exceeds demand, grid operators face a choice between curtailing excess supply and balancing loads. The latter can be executed through either dispatchable generation or diversion of the excess electricity into various forms of chemical, mechanical, or thermal storage (Hauch et al., 2020). As a molecular carrier for stored chemical bond energy, liquid hydrocarbon fuels serve as a demand-side management (DSM) option and portable energy bank in hard-to-electrify transportation modes such as aviation. The e-SAF production train in fact serves multiple sectors at once: every batch of hydrocarbons passes through post-FT distillation, where it is separated into fractions from renewable diesel down to naphtha.

The current literature on techno-economic estimates of e-SAF primarily examines the fuel production chain in isolation and assumes current electricity grid mix within a demand-driven configuration. Some studies incorporate predictions of declining grid carbon intensity (CI), and a handful investigate the price dynamics of on-site renewables installations, but very few set out to test hypotheses of how the production economics would play out under a radically transformed VRE-flexible-demand system, a hypothesis originally considered and partially assessed in EDF's High-Integrity SAF Handbook, Appendix E (Piris-Cabezas, 2022). Our paper is unique in stressing the grid-balancing role of PtL *under a supply-driven VRE system*. As such, the consequent assumptions inform our results that show significant cost savings compared to most other techno-economic analyses. Ours is one of the first studies to combine supply-driven renewables-based grid optimization with a techno-economic analysis of e-SAF production from excess power within a flexible demand system, and the first focusing on aviation.

In this analysis we investigated the following: Is e-SAF deployment at national scale physically and economically feasible in the U.S., given a defining characteristic of interoperable demand that balances variable renewable electricity supply? How do cross-sector synergies between aviation and the power grid impact cost competitiveness systemwide – notably e-SAF production cost; power supply curtailment; and required grid capacity for generation, backup, & storage?

We also test the impact that operating e-SAF production on an interruptible basis could have on its cost competitiveness, estimate present and future e-SAF costs under varying power grid conditions and fuel technology choices, and compare with biogenic SAF production costs.

We find that synergies dramatically bring down costs for both aviation fuel and power sectors; moreover, SAF volume targets on the order of billions of gallons like in the U.S. can be met by the quantities of surplus renewable electricity that emerge as a byproduct of VRE expansion over the coming two and a half decades. We also find that e-SAF pathways can unlock significant cost savings in the near- to mid-term and become cost competitive with other alternative fuels such as biofuels.

The rest of this paper is organized as follows. Section 2 describes the interaction of e-SAF manufacturing with the power sector's energy transition in further detail. Section 3 provides greater

insights into the mainstream e-SAF process modules. Section 4 describes our methods, covering the modeling frameworks, associated assumptions, data and scenario construction. Section 5 presents our results. Section 6 describes the caveats of the analysis. Section 7 concludes with a brief discussion of policy implications.

2. Interaction of e-SAF manufacturing with the power sector's energy transition

The electricity needs of all e-fuel routes are substantial enough for electricity to be considered a feedstock itself. One unit of e-fuel energy requires an input of around two units of energy for the solid oxide electrolysis cells (SOEC) route (Malins, 2017) and more than two units for some cases like the proton-exchange membrane electrolysis cells (PEMEC) reaction route (Adelung, 2021). Irrespective of technology, the energy sources must be renewable for the finished e-fuel to render a real climate benefit. Therefore, integrated power system planning for e-fuel production must avoid spiking electricity spot prices or cannibalizing baseload capacity intended for the local utility's own transition away from fossil generation (Pio et al., 2023). Fortunately, there are geographies where this is already realistic and attainable. Untapped potential of renewable resources around the world provides the opportunity to build synthetic fuel plants where renewable energy is cheap and abundant (Fasihi et al., 2016; König et al, 2015; Sherwin, 2021).

In demand-driven electric power systems, the challenge of excess VRE generation is typically addressed rigidly by curtailment, whereby electricity output is deliberately reduced such that supply accommodates the demand profile. In contrast, grid balancing in a supply-driven system strategically employs a suite of flexible demand options to match supply. However, once large shares of wind or solar capacity are in place, power production becomes intermittent, and the ability to manage the demand response becomes a critical feature for balancing the grid. Unlike demand-driven systems, renewables-based power generation systems are supply driven and can operate without significant energy storage while still providing a high level of reliability (Lugovoy et al., 2021).

In this context, a significant fraction of demand would need to be flexible, making interruptible technologies like electrolyzers essential to facilitating a comprehensive energy transition, rather than adding pressure to finite infrastructure capacity. E-fuel production facilities can be designed to take dynamic loads or have the flexibility to operate the electrolyzer in reverse as a fuel cell to generate electricity when necessary, further enhancing its grid balancing services (International Renewable Energy Agency [IRENA], 2019; Schmidt et al., 2017).

Hydrogen production from proton-exchange membrane (PEM) and solid oxide electrolysis is flexible due to its virtually instant ramping speed and ability to store hydrogen as a back-up energy supply (IRENA, 2018; IRENA, 2019; IRENA, 2020). This makes e-fuel production facilities particularly well suited to balance grids with a high share of renewable electricity, both instantly and across seasons. Our analysis inquires as to the magnitude of surplus VRE involved in this role, if directed toward aviation uses. Our model specifies that any watt-hours used for electrolytic hydrogen must have a direct physical connection (from power source to electrolyzer) and must not detract from fulfilling baseload needs, in line with additionality, time-matching, and deliverability principles that ensure hydrogen is produced and managed as responsibly as possible throughout its supply chain for maximum climate benefit (Ocko and Hamburg, 2022; Sun et al., 2024).

Intermittency at the e-SAF facility raises competing considerations between fixed costs and variable, or production-dependent, costs. VRE-based power systems span a broad range of flexible demand types according to their load factors, even as high as 70% (König et al., 2015). While operating with lower capacity factors increases the capital and fixed operational and maintenance costs, it can significantly lower the renewable electricity contract prices as compensation for the inconveniences of variable availability and for the customer's *de facto* providing grid balancing services back to the electricity supplier. As energy expenses are the major contributor to the overall fuel production costs, this opens the door to significant cost savings, provided countries deliver on the transformation of their power generation systems. Such conditions enable e-SAF pathways to become cost-competitive sooner than anticipated vis-a-vis market-mature alternative jet fuel pathways such as HEFA-SPK.

Additional e-SAF production cost savings emerge from harnessing thermodynamic efficiencies as well as other potential synergies between high-temperature co-electrolysis, liquid solvent-based DAC technologies, water desalination and the exothermic FT reaction. By capitalizing upon synergies within the production pathway and with transition developments in the power sector, DAC e-SAF deployment could happen earlier as their abatement cost would be competitive with alternatives sooner than anticipated (see Section 5, Figure 5). Furthermore, our results show that when SAF pathways are assessed based on abatement costs, e-SAFs have a far more cost-efficient price per ton of CO_2 abated than other pathways (see Section 5, Figure 6*)*. This is particularly noteworthy for a jurisdiction like Europe, where an EU ETS allowance price of €100/tCO_2 is a real possibility and would provide a sufficient incentive to cover the future abatement costs for e-SAF.

3. Mainstream e-SAF routes

The process train for e-SAF pathways consists of four main components: obtaining CO_2, splitting or activating CO_2 into CO, splitting water to obtain H_2, and sending the syngas mixture of H_2 and CO through FT synthesis to form long-chain hydrocarbons (Figure 1). Conventional FT reactors, already in use for decades as a mainstream industry component, can be tuned to maximize the output share of individual target products. The spectrum of products is distilled and refined by carbon backbone lengths; hydrocarbons isolated in the range C8 to C12 are typically most suited for jet fuel as a replacement to conventional kerosene.

Two routes have received notable attention in literature, given their stage of technological development and ease of scaling via modular units:

1. The low-temperature route, which uses proton-exchange membrane electrolysis cells (PEMEC) to obtain electrolytic hydrogen, with options to procure CO_2 either by purchasing point-source capture (PSC) CO_2 from a neighboring industrial facility or through a low-temperature solid sorbent DAC unit integrated on-site with the fuel synthesis equipment. This CO_2 is activated to carbon monoxide in a reverse water-gas shift (RWGS) reaction or equivalent, and the syngas is fed into the FT synthesis reactor.

2. The high-temperature route, which relies on solid oxide electrolysis cells (SOEC), a versatile stack type that can electrolyze inputs either independently (steam $\rightarrow H_2$, or $CO_2 \rightarrow$ CO) or together. Here we assume that the SOEC unit co-electrolyzes steam and CO_2, tuned to produce the syngas at

optimal stoichiometric ratio for the subsequent feed into the FT reactor (Dittrich et al., 2019). This route also takes two options for CO_2 sourcing, either purchased from PSC or using a high-temperature aqueous solvent DAC unit at the e-SAF facility. Without the need for an intermediate CO_2 activation step (RWGS), the high-temperature route modeled in our analysis possesses a reaction stoichiometry that requires only 2/3 as much H_2 as the low-temperature route.

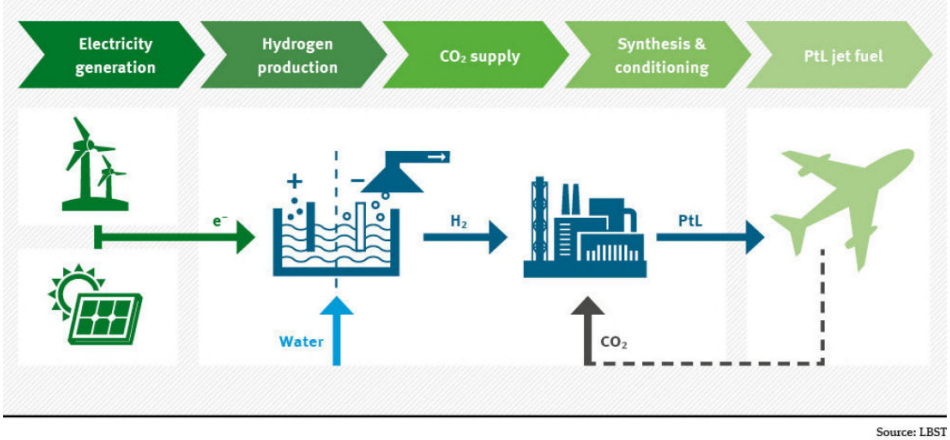

Figure 1. Generic schematic of power-to-liquid (PtL) process train components: the hydrogen and carbon molecular carriers for the FT reaction are obtained separately, then conditioned and combined into a syngas mixture of H2 and CO. The CO_2 input can draw from a variety of sources for which the CO_2 molecules would otherwise have persisted in the atmosphere. Thus, the PtL process is carbon neutral. Figure from Schmidt et al. (2016)

3.1 e-SAF process modules

This section explores the key modules of the e-SAF process: manufacturing green hydrogen via renewable-powered electrolysis, sourcing and activating CO_2, and converting syngas to liquid fuels through FT synthesis.

3.1.1 Manufacturing green hydrogen

Water electrolysis technologies accomplish the redox reaction through various types of charge carriers, or electrolytes, and their respective electrode arrangements. Of these designs, the three most suited to fuel production and most highlighted in the literature are alkaline electrolyzer cells (AEC), PEMEC, and SOEC (IRENA, 2020; Schmidt et al., 2016; Fasihi et al., 2016; Dieterich et al., 2020; Schmidt, et al., 2017; Küngas, 2020).

Given the span of options for process units forming the e-SAF train, the optimum configuration in terms of energy expenditure, monetary cost, and physical feasibility will be site-specific depending on the unique combination of local factors. Alkaline and PEMEC electrolysis, also referred to as low temperature electrolysis (LTE), operate around 80-100°C and feature in most industrial applications today (Schmidt et al., 2017). SOEC electrolysis, also known as high-temperature electrolysis (HTE), commonly operates in the range of 600°C– 800°C and is not yet widely commercialized (Malins, 2017).

In the near term, before solid oxide stacks are fully demonstrated and proven in operational environments, higher technology readiness levels (TRL) may favor membrane LTE over solid LTE (Schmidt et al, 2016). LTE typically does not need input heat, as its thermal demand is satisfied internally by exchangers reclaiming resistive losses at the electrode stack (Peterson et al., 2020b). However, linking LTE with upstream DAC likely requires LT-DAC, the less energy-efficient of two primary DAC technologies.

Despite its lower TRL, high-temperature co-electrolysis has a higher electrical efficiency than its low-temperature counterparts, exhibiting fewer resistive losses, lower cell voltage, and higher current densities (Küngas, 2020). HTE's operating temperature also is comparable to that of HT-DAC output gases (800°C -900°C), eliminating the need for the gas compressors and coolers in DAC equipment integrated with fuel synthesis described in Keith et al. (2018).

In configurations without a DAC unit integrated on-site, the SOEC route can function as a heat sink for thermal integration to tap energy from the highly exothermic FT reaction, bringing down the operational costs of the electrolyzer and therefore the entire process train (Malins, 2017; Dieterich et al., 2020). This heat sink is not available at the PEM stack in the low-temperature configuration. Therefore, where and when DAC is not feasible to incorporate into the production train, pilot e-SAF facilities will likely find thermodynamic integration and its associated opex savings more accessible using the SOEC route.

In addition, direct electrochemical conversion of CO_2 into CO – particularly co-electrolysis in a single step alongside H_2O - is advantageous for paring down the number of process steps involved and removing chances for selectivity losses to deplete the pathway's overall caloric conversion efficiency (Sheehan et al., 2018; Adelung et al., 2021). SOEC is the most mature technology today for direct electrochemical conversion of CO_2 into CO (Hauch et al., 2020).

Although AEC is the most widely used today, our modeled routes do not employ AEC as its lower current density results in higher operational costs and lower H_2 purities (Pio et al., 2023). This cost differential is tolerable for some industrial processes that use relatively small amounts of H_2 but less suitable for the massive amounts of hydrogen feed involved in e-SAF production. Furthermore, AEC has a narrower range of tolerance for operating at variable loads (Pio et al, 2023).

Of the cost factors in e-SAF conversion, capex is dominated by energy expenses – therefore, industrial designs that take advantage of inexpensive power, streamlined energy efficiency, and thermal synergies all have a sizeable bearing on the electrolysis segment of e-SAF economics. Precise industry cost data for electrolyzers is often kept confidential (IRENA, 2020). Recent U.S. Department of Energy (DOE) estimates report hydrogen costs around \$2-7 /kgH_2 using National Renewable Energy Laboratory (NREL)'s Hydrogen Production Analysis model, version 3.2018, a discounted cash flow model with a transparent breakdown of process design assumptions and a consistent cost analysis parameters (Peterson et al., 2020a & 2020b).

The electricity price at any given installation depends on a range of location- and time-dependent variables, including the local status of renewables deployment and the negotiated purchase agreement between the industrial customer and the utility retailer. That said, a feature critical to minimizing

energy costs is that electrolyzers, unlike FT units, have the ready flexibility to react to intermittent renewable electricity generation by rapidly changing their on/off operating state, some in a matter of milliseconds (Hauch, et al., 2020). This will allow for demand-side calibration of electrolysis operation schedules according to electricity availability and price: ramp up production when renewable electricity is cheap and abundant; ramp down production when renewable electricity is scarce and more expensive (Hauch et al., 2020).

3.1.2 Sourcing and activating CO_2

When not operating on externally purchased CO_2 feed, the e-SAF synthesis facility takes CO_2 from an integrated DAC unit. The diverse array of DAC technologies have in common a basic operating sequence: bind dilute CO_2 from a moving air current, recover the CO_2 in concentrated form, and then regenerate the sorbent or solvent. The two most developed types are high-temperature liquid solvent and low-temperature solid sorbent DAC (McQueen et al., 2021; Fasihi et al., 2019).

A high-temperature aqueous solvent process, such as one developed by Carbon Engineering, absorbs CO_2 using a strong basic hydroxide solution in a pair of continuous loops. Anionic exchange liberates the CO_2, regenerates the sorbent, and sends the trapped CO_2 in salt pellet form through drying and calcination, which liberates the CO_2 at an operating temperature around 900°C (Keith et al., 2018). Carbon Engineering's pilot innovation development plant in Squamish, British Columbia has a 350 tCO_2/yr capacity (Ozkan et al., 2022).

A low-temperature solid sorbent unit uses an amine-based contactor to adsorb and desorb CO_2 in a batch process switching back and forth between capture and release modes, also known as temperature vacuum-swing adsorption. Steam in the 100-130°C range flushes the CO_2 off the contactor surface to a recovery stream and regenerates the sorbent material (Deutz & Bardow, 2021). Climeworks and Global Thermostat have opened demonstration LT-DAC plants on the order of 1000 tCO_2/yr (McQueen et al., 2021).

The different temperature requirements of liquid solvent DAC systems and solid sorbent DAC systems translate into different energy contributions to opex, (when thermal needs are not met by free-of-charge waste heat.) Contactor airflow geometry and capture performance of the binding substrate/medium are also influential design elements in the levelized costs of DAC (LCOD) (NASEM, 2019; McQueen, et al., 2021; Fasihi et al., 2019).

Overall LCOD for pilot plants range anywhere from \$60/tCO_2 to over \$1000/tCO_2 (NASEM, 2019), even up to \$3100 (Young et al., 2023), depending on variations in technology type, energy efficiency, and utility prices. N^{th} plant LCOD figures converge in the \$100-200/tCO_2 range as modular learning scales and energy cost burden falls, with some optimistic cases reaching ~\$30/tCO_2 (Sabatino et al., 2021; Breyer et al, 2019; Fasihi et al, 2019).

The wide range underscores the importance of checking analytical assumptions in techno-economic analyses, translating them to a site's specific context, and subdividing e-SAF pathway evaluation into separate routes with fundamentally different technology configurations.

3.2.3 Syngas to liquid fuels

The FT synthesis reaction itself is well established at industrial scale with modest energetic needs and straightforward to operate so long as syngas is ready to feed in (Pio et al., 2023; Terwel & Kerkhoven, 2018). Capex estimates for FT reactors range between EUR 400-1300 per kW of output fuel (Malins, 2017). Completing the power-to-liquids process train requires that CO_2 be reduced to its chemically activated form, either during co-electrolysis alongside water or in a separate reaction step such as RWGS (Rojas-Michaga et al., 2023). The RWGS reaction has been demonstrated in industrial environments, but work remains to scale its volume (Schmidt et al., 2016).

For this step in the e-SAF process train, industrial equipment can be repurposed from conventional FT operations, and shared with new bio-SAF pathways that generate CO_2 byproducts (Pio et al., 2023). These interconnections may help to bridge capital costs of e-SAF installation buildout in the near term.

Exothermic reaction characteristics (ΔH = 165 MJ/ kmol CO reacted) offer "waste" heat to be recycled into the previous process steps. In certain configurations like the representative HT and LT routes modeled in our study, the linked process units transfer enough heat to cover all the other steps without combusting any of the FT hydrocarbon co-product output. Otherwise, as is frequently done in industrial manufacturing, the light ends (CH_4 and naphtha) are fed back into combustion furnaces for process heat, and the only loss to the facility is the revenue that would have been obtained from selling the co-products to power combustion heat elsewhere. For instance, a group at Universitá Perugia modeled a SOEC-to-FT process that internally satisfies the entire thermal needs of its electrolysis stack using recycle loops, heat exchangers, and a gas-fired furnace consuming roughly 7% of the FT output slate (Cinti et al., 2016).

4. Methods

First, to assess the cross-sector synergies between aviation and the power grid impact cost competitiveness systemwide, we examine the techno-economics of two e-SAF routes assuming surplus renewable electricity as energy source. The modeled e-SAF routes in this study were configured based on energy conversion efficiency, versatility for modular integration, suitability to variable load operation, and technology readiness. The estimates are based on data from a variety of sources across academia and industry, described in Section 3 and next. Variable and fixed costs at each process step have already been levelized prior to incorporation into our model. These are then compared to costs of gasification-Fischer-Tropsch, alcohol-to-jet, and HEFA-SPK pathways. The assumptions are described in Section 4.1.

Second, to assess whether e-SAF deployment at national scale is physically and economically feasible in the United States, we quantify the scale of potential annual surplus renewable energy in the conterminous United States when the decarbonized power sector employs PtL as a DSM option. We compute these estimates using the open-source United States Energy SYStem (USENSYS) optimization model.

The model runs in our study assume a gradual transition to a renewables-based electric power system in the U.S. through 2050. The reference case illustrates the state of the power grid without PtL, and three flexible-demand scenarios test the effects of varying the power prices and the minimum required load

factor for electrolyzers to operate. These effects include efficiencies conferred to the grid structure in terms of installed capacity and associated storage required to fulfill future power needs.

To understand how the scale-up of DAC e-SAF could help balance an increasingly decarbonized power grid, we also evaluate the impact of electrolysis on grid operation characteristics, e.g. energy storage requirements and curtailments. Generation and storage technologies include centralized wind, solar, hydropower, geothermal, nuclear, distributed generation (technology neutral), intermittent PtL, battery storage, and pumped hydro storage. The model and the underlying database are described in Section 4.2.

4.1 Power-to-liquid cost assumptions

The fuel production estimates are derived from a sum of levelized discounted cash flow (DCF) costs at each process step (CO_2 procurement, electrolysis, CO_2 activation, and fuel synthesis) as follows:

$$Levelized\ cost\ of\ Hydrocarbon = cost_{CO_2} + cost_{H_2} + cost_{syngas-activ} + cost_{FT}$$

Variable costs per unit of output fuel respond to reaction stoichiometry, as feed stream material costs comprise the bulk of opex. Most of the reactants can achieve a near-100% mass conversion over multiple passes with recycle loops.

For simplicity, it is assumed in this model that the mix of FT hydrocarbon lengths in the product slate sell for the same price. Therefore, the relative weights of revenue per unit fuel by fuel type do not affect the kerosene share of net dollar cost. Empirical data have reported from about 20% to 60% kerosene-range fractions in the FT product slate depending on which size of hydrocarbon the optimization targets (WEF, 2020; Schmidt et al., 2016); one industry manufacturer reports tuning the reaction to output upwards of 80% kerosene (Bekoe, 2023).

Opex and capex for distillation and post-processing are not included in this study, as they do not have a major influence on total cost.

The component cost data are obtained from: National Academy of Sciences and industry developers' literature for DAC; IEA reports for other purchased PSC carbon prices (IEA 2021b); DOE-NREL for H_2 production costs (Peterson et al., 2020a & 2020b); Clean Skies for Tomorrow (CST) for FT and RWGS reaction costs (WEF, 2020); and S&P Global for the fossil jet fuel benchmark price (Platts, 2024).

The comparison against other pathways is based on biofuel production costs and achieved CO_2 abatement values from ICAO "SAF Rules of Thumb" (ICAO, 2022) and the ICAO document "CORSIA Default Life Cycle Emissions Values for CORSIA Eligible Fuels" 3rd Edition (ICAO, 2021).

The base case for both high-and low-temperature routes takes key assumptions from NREL's electrolysis specifications for a 50,000 kgH_2/day installed capacity, combined with FT (and RWGS in the PEMEC case) reference costs from CST-WEF. Using the Hydrogen Production Analysis discounted cash flow model, version 3.2018, NREL reports present a transparent breakdown of electrolytic hydrogen cost factors, including both electric and gas input energy specifications, for a consistent cost

analysis methodology across the parameter space. CST reference costs draw insight from proprietary industry data. Platts jet fuel price benchmark prices (global average $780 in 2024) combine IATA and S&P data to report regional and world prices.

We then iterate on both the current and future technology configurations by changing the load factor and power price for the electrolysis operator to demonstrate the potential cost effects of varying these parameters in a flexible supply-driven power structure.

Next sub-sections provide further details on CO_2 input cost assumptions (Section 4.1.1) and the cost savings associated with thermodynamic synergies of co-located process modules (Section 4.1.2). Finally, Sections 4.1.3 and 4.1.4 describe the base case scenario, and the flexible power demand scenarios for a range of load factors and power input cost, respectively.

4.1.1. CO_2 input costs

CO_2 prices from different capture sources vary according to CO_2 purity. For purchased CO_2 captured at other industrial point sources (Table 1), we take dilute stream prices of $90 (current) and $50/$tCO_2$ (future) and concentrated stream prices of $35/tCO2 (current) and $15/$tCO_2$ (future) from literature ranges (Fasihi et al., 2019; Malins, 2017; IEA, 2021b; WEF, 2020). The capture energy costs are already borne by the retailer, and the e-SAF facility expends no additional process energy.

Table 1. Industrial point source capture (PSC) CO_2 prices in $/$tCO_2$ from dilute (fossil-based power generation, iron, steel, etc.) and concentrated (ethanol fermentation, pulp and paper boilers, natural gas pre-combustion cleaning, etc.) sources.

Industrial PSC *(*$/$tCO_2$*)*	Now	Future
Diluted	90	50
Concentrated	35	15

For fuel production routes using on-site integrated DAC, we partition expenses into energy costs and balance of costs (Table 2), to reflect their differing causes of variability. The energy share of input variable costs is highly sensitive to PPA prices, while the other variable and fixed DAC costs are not. The energy demand is on the order of 5 MWh/tonne fuel, and we define the input energy to come from entirely renewable or internal waste sources. For capex, we use literature mid-range values. Estimated LCOD ranges in literature reviews largely take capital and energy bases from Carbon Engineering and Climeworks for HT liquid solvent and LT solid sorbent types, respectively.

Carbon conversion of the overall fuel production train is 95.5% by mass after purges and losses (WEF, 2020).

Table 2. Representative levelized cost of DAC (LCOD) for high- and low-temperature technologies, based on industry techno-economic estimates. 'LCOD without energy' consists of capex and fixed O&M. FT heat integration reduces total input energy requirements by ~900 kWh/tCO_2 (own calculation). 'First plant' represents technology in the current decade, while 'nth plant' is around year 2035/2040.

a: (NASEM, 2019)
b: (Keith et al., 2018)
c: (Fasihi, et al., 2019)
d: (Deutz & Bardow, 2021)
e: (Beuttler et al., 2019)

		Unit	First plant	n^{th} plant
HT liquid DAC	LCOD without energy	$/$tCO_2$	190[a]	100[a]
	Energy demand (electric + thermal)	kWh/tCO_2	2580[a]	1540[b,c]
	Energy demand with FT heat integration	kWh/tCO_2	1687	647
LT solid DAC	LCOD without energy	$/$tCO_2$	250[a]	100[a]
	Energy demand (electric + thermal)	kWh/tCO_2	3410[d]	2000[c,d,e]
	Energy demand with FT heat integration	kWh/tCO_2	2517	1107

4.1.2. Thermodynamic synergies for co-located process modules

The exothermic FT reaction generates input process heat for the DAC units. When waste thermal energy is transferred directly via heat exchangers without temperature upgrading, around 90% can be reclaimed (Sherwin, 2021). Assuming the FT reaction gives off 165 MJ/ kmol CO reacted, and the system has a 95.5% carbon mass conversion (with the remainder 4.5% purges and losses), there is 2.9 MWh of recyclable heat per tonne of fuel synthesized. In the high-temperature route, this ΔQ provides 35% energetic savings on the DAC component today and 60% in the future. In the low-temperature route, this ΔQ provides 26% energetic savings today and 45% in the future.

The medium-grade FT process heat at ~300° C most conveniently transfers to the process modules operating at temperatures below 300° C, namely saltwater desalination and solid LT-DAC. Meanwhile, high-temperature process units operating around ~700-900 °C can also make use of the FT thermal energy for preheating reactants and boiling water.

High-temperature route, DAC to SOEC: The thermal energy feedstock for SOEC (6% of H_2 cost in NREL's base case) can be neglected when HT-DAC, SOEC, and FT modules are connected in the process train. Hot captured gases released from the calciner at 800-900°C, consisting primarily of CO_2 and H_2O vapor, are fed directly to the electrolysis stack and to heat exchangers vaporizing the additional H_2O required for the electrode reaction's stoichiometric ratio.

Low-temperature route, DAC to RWGS + PEMEC: Electrolysis at 80-100°C requires low-grade warming of the ambient temperature feed stream. Under NREL's cost model, the heating to 100°C is not explicitly enumerated, as this heat is satisfied internally by resistive losses at the electrode stack. DAC on a temperature vacuum-swing adsorption cycle does require thermal inputs, which are covered in part by FT waste heat. RWGS typically operates around 800°C.

4.1.3. Base case assumptions: rigid load

PEMEC operates at 97% capacity factor of its installed 119 MW; SOEC operates at 90% of its 80MW installed capacity. Whereas SOEC stack temperature is 800°C (offering a heat sink for process train integration), PEMEC stack temperature ranges 80-120 °C with thermal needs satisfied by recycling within the electrolytic module. All capital costs for the stacks assume manufacturing at volumes such that economies of scale have been achieved.

Without any cross-sector synergies, the electrolysis facilities operating on static demand-driven power structure must pay premium rates for baseload power supply. Effective electricity cost over the 40-year lifespan of the plant was defined at 7.35 ¢/kWh (current) and 7.91 ¢/kWh (future). While maximizing the fraction of full-load hours optimizes the capital investment, and near-steady-state operation streamlines equipment maintenance, the requisite operating costs of such an electricity-intensive reaction are a function of the grid power purchase agreement (PPA) price for constant supply. As such, the baseline e-SAF costs using dilute industrial PSC CO_2 are $1734/tonne and $2650/tonne for high- and low-temperature routes.

4.1.4. Flexible power demand at 75%, 50%, 25% load assumptions

To test renewable power sector surplus capacity, we illustrate scenarios with electrolyzers to represent flexible demand for electric power at specified annual load requirements, with notional electricity prices for interruptible grid contracts. For 75%, 50%, and 25% load, the respective prices are set at $15/MWh, $10/MWh, and $5/MWh. These are lower than the LCOE of $55/MWh estimated by a USENSYS baseline run: the electrolysis operator pays markedly less than what an average grid user would pay for full-time power supply.

The electrolyzer runs intermittently on the defined load factors, while the DAC unit, RWGS reactor, and FT reactor are all assumed to run at steady state. An H_2 buffer stores the reaction intermediate as needed to facilitate the modular connection between electrolytic output and syngas conditioning.

While DAC poses a nontrivial energy demand, existing waste streams of CO_2 delay the necessity of DAC until future decades when the grid will be largely decarbonized and able to deliver full-time, low-cost renewable energy. The DAC carbon source is portrayed here in current as well as future fuel costs for representative purposes.

4.2 Power sector transition

To simulate the performance of the United States electric power system over the course of the energy transition, we apply a high-resolution, open-source capacity expansion model drawing from PowerGenome source data. PowerGenome is an open-source data management library with a database that provides snapshots of power sector infrastructure characteristics and policy constraints at queried future timepoints up to 2050 (Schivley, 2024).

Our least-cost optimization model USENSYS solves with perfect foresight and reports the power sector profile at three decadal waypoints, 2030, 2040, and 2050. Outputs depict changes over time of generating and storage capacity, transmission capacity, curtailment, and bidirectional operation of electrolyzers as feedstock producers for either power-to-liquid conversion or hydrogen fuel cells. Grid

operating conditions over the weather-year are computed at a resolution of 24 hours per day, across 52 weeks or 364 days.

Next sub-sections provide further details on PowerGenome's database (Section 4.2.1), the exogenous constraints necessary to ensure the decarbonization of the grid by 2050 (Section 4.2.2), and the estimates for power drawn in the PtL process to translate the total surplus electricity into an estimate of nationwide fuel potential (Section 4.2.3). Finally, Section 4.2.4 describes the scenarios modelled.

4.2.1. Source data

In PowerGenome, clusters of individual generation sites are grouped into 26 market regions based loosely on EPA's Integrated Planning Model regions. These reflect administrative structures of independent system operators and regional transmission organizations that handle power generation, delivery, and prices. Costs of new-build generators and permittable generation sites are taken from NREL's Annual Technology Baseline. The database creates model inputs for roughly 1500 renewable technologies, clustered by location. The generation technologies include centralized solar photovoltaics, distributed generation, onshore and offshore wind turbines, geothermal, nuclear, and hydropower. Each "cluster" is represented by its own unique hourly generation profile, in terms of capacity factors, based on historical weather data. Storage options are battery and pumped hydropower, and the interregional transmission network is allowed to grow to a maximum of ten times the initial capacity.

PowerGenome's base year renewables generation capacity in 2023 is calibrated to Catalyst Cooperative's Public Utility Data Liberation database, a translation of the U.S. federal Energy Information Agency dataset. The base year demand profile is taken from NREL EFS and FERC 714 datasets, which provide hourly demand by sector and subsector. Future year load curves include new demand from vehicle and building electrification. As such, the national total demand of 4517602 GWh grows to 5916446 GWh in 2040, and 6963840 GWh in 2050 (PowerGenome). Regions with the highest load are TRE, PJME, SRSE, PJMW, FRCC, which correspond to Texas, Mid-Atlantic, Southeast, Ohio Valley, and Florida, respectively.

4.2.2. Exogenous constraints

The representative net-zero scenarios simulate new-build renewables and storage at the requisite scale to satisfy national baseload each year and fully decarbonize the grid by 2050. Existing 2023 generation and storage infrastructure contributes to total capacity during the transition period but is assumed to retire by 2050. In our scenario definitions, we do not allow new investment in fossil generation, and we restrict early nuclear retirement to encourage decommissioning of fossil infrastructure instead. Furthermore, pumped hydro storage, hydropower, biomass, and nuclear capacity are capped at existing levels. The threshold marginal price of electricity is set at $10 000/ MWh. We limit backup capacity to illustrate grid planning that minimizes reliance on dirty fossil-fired peaker plants.

4.2.3. Electrolytic hydrogen-based e-SAF potential assumptions

Estimates for power drawn in the e-SAF process train appear in Table 3. We use these to translate the usable surplus electricity into an estimate of e-SAF potential, supposing a majority jet-fuel product slate. Electric demand is defined as follows:

$$\text{Electric demand} = el_{DAC} + el_{H2} + el_{RWGS} + el_{FT}$$

Where el_k is the electric demand of component k. RWGS and FT electric demand are nonzero but small relative to the power drawn by DAC and electrolysis. Therefore, we treat RWGS and FT energy cost as part of the fixed opex bundle rather than modeling their specific price impact.

Table 3. Energy demand of high-temperature and low-temperature routes of the DAC to FT power-to-liquid pathway. The electricity needs of each component are a function of the state of technology at given year. "First plant" represents technology in the current decade, while "nth plant" is reached by 2040. The right-most columns refer to the full fuel process train when CO_2 is captured on site; the power needs comprise both electrolytic and DAC steps. When CO_2 is bought from point capture, on the other hand, the electric demand is only the electrolysis portion in the center columns.

		First plant	nth plant		First plant	nth plant		First plant	nth plant
	HT liquid DAC			***HT-SOE***			***Full train DAC-to-FT***		
Original energy demand (electric + thermal)	kWh/ t fuel	8420	5030	kWh/ t fuel	11800	11000	MWh/ t fuel	20.3	16.0
Energy demand with FT heat integration	kWh/ t fuel	5510	2110	kWh/ t fuel	11800	11000	MWh/ t fuel	17.3	13.1
	LT solid DAC			***LT-PEM***			***Full train DAC-to-FT***		
Original energy demand (electric + thermal)	kWh/ t fuel	11100	6530	kWh/ t fuel	25000	23000	MWh/ t fuel	36.1	29.6
Energy demand with FT heat integration	kWh/ t fuel	8210	3610	kWh/ t fuel	25000	23000	MWh/ t fuel	33.2	26.6

4.2.4. Scenarios

The REF_ZERO scenario simulates the electric power system without PtL synergies. This provides initial reference quotes of the renewable generation, storage, transmission, and backup capacity required for a zero-carbon electricity power system.

Three additional scenarios build upon REF_ZERO with the added option to invest in hydrogen production. In PTL25H05D (PTL with 25% Load Factor for Hydrogen production capacity and a cost of electricity of 0.05 USD /kWh), the minimum load factor for electrolysis to operate is 25% of annual hours. In PTL50H05D, the minimum load factor is 50%.

For both these scenarios, we set the initial cost of electricity for electrolysis users at $5 /MWh (0.5 ¢/kWh), declining over the two decades inversely to the total demand. This PPA contract price enables competitiveness against other technologies since it is below levelized electricity costs (which start at roughly $50/MWh in early years). It also averts distorted incentives that would drive new installations of baseload generation capacity solely to sell to electrolysis users. From the combined system

perspective, electricity sold to hydrogen producers is considered as a credit against losses. This allows VRE builders to install sufficient generation capacity to meet the base load requirements and still earn revenue during off-peak hours, and in so doing reduce storage requirements and improve grid stability.

PTLH05D2W illustrates an additional option for grid flexibility in two-way operation of electrolyzer stacks. For the forward reaction of water to hydrogen, all three load levels are in play at different electricity prices: electrolysis at 25%, 50%, and 75% utilization earn the grid a credit of 0.5, 1.0, and 1.5 ¢/kWh respectively in year 2030, similarly declining over time over the two decades inversely to the total demand. For the reverse reaction of hydrogen to backup electricity, the power price is set at $140/MWh. Caloric conversion efficiency is defined at 70% in both directions.

The difference in outputs between REF_ZERO and the three other scenarios tests the potential magnitude of surplus VRE for e-SAF production and the effectiveness of this DSM measure for streamlining grid operation, in terms of capacity and transmission savings along with avoidable curtailment.

Curtailed electricity supply amid variable weather patterns is an inherent feature of high-renewables systems with rigid demand, as illustrated in REF_ZERO. When both supply and demand are predefined by external factors, the only balancing options are energy storage or back-up generation. Therefore, to meet the total demand, the model must scale up either installed baseload generation capacity (which leads to overproduction and frequent curtailment) or time-shifting storage capacity. In contrast, when demand is flexible, the model has more options, including: scale up baseload capacity and use electrolyzers to "absorb" the excess electricity during off-peak hours; or replace battery storage with electrolytic H_2 that delivers power back to the grid via fuel cells during hours of high demand.

5. Results

5.1. Production cost of electrolytic hydrogen-based e-SAF

Levelized cost of production for e-SAF should become much more affordable over the span of two and a half decades, given (1) the dramatically declining LCOE anticipated with the transformation of renewable power sector, and (2) the technological learning curve that still lies ahead for e-SAF production components. Even the first decade will bring noticeable gains in VRE availability if the pattern of grid expansion in recent years continues (IEA, 2021a; Seymour et al., 2024). Switching from static to flexible demand already brings at least 14% and as much as 45% cost reductions through facilitating lower power prices (Figures 2 and 3). These savings are sufficient to compensate for the rise in levelized capex under the load conditions in all three of the modeled cases.

Between the high-and low-temperature routes, the SOE route's lower stoichiometric H_2 requirement spurs cost savings over PEM routes.

Although LT-solid tends to require more kWh overall than HT-aqueous DAC (Fasihi et al., 2019), a larger share of LT-solid DAC energy demand can be readily satisfied by internal recycling of waste heat and mass carriers. LT-DAC more readily accepts waste heat from other industrial processes due to its lower operating temperature, and its modular design more readily lends itself to transposition onto various plant sizes (Young et al., 2023).

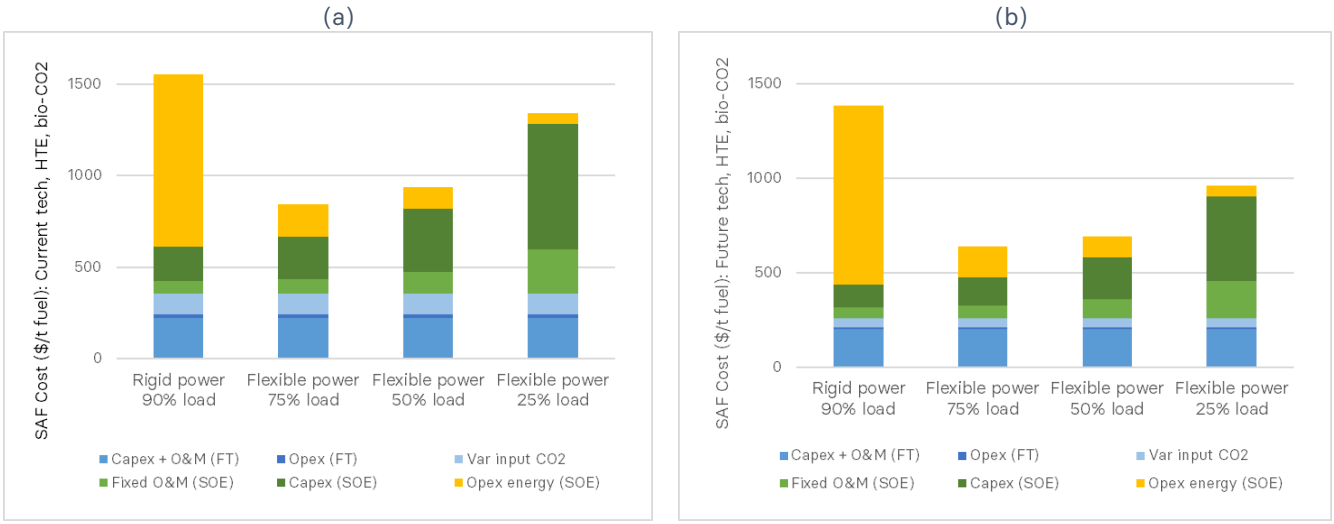

Figure 2. Cost breakdown of the high-temperature SOEC (SOE) route, taking purchased biogenic CO_2 feed, with (a) current and (b) future technology. Energy feedstock accounts for 61-68% of the total fuel cost when baseload electricity prices are high. Intermittent electrolyzer operation at lower load factors raises capex but allows for lower negotiated electric rates, causing energy feedstock opex to decrease accordingly, to 26% of total fuel cost or below. The FT reactor operates at steady state and sees no change in power prices or capex. Among these representative scenarios, total cost is lowest at 75% load.

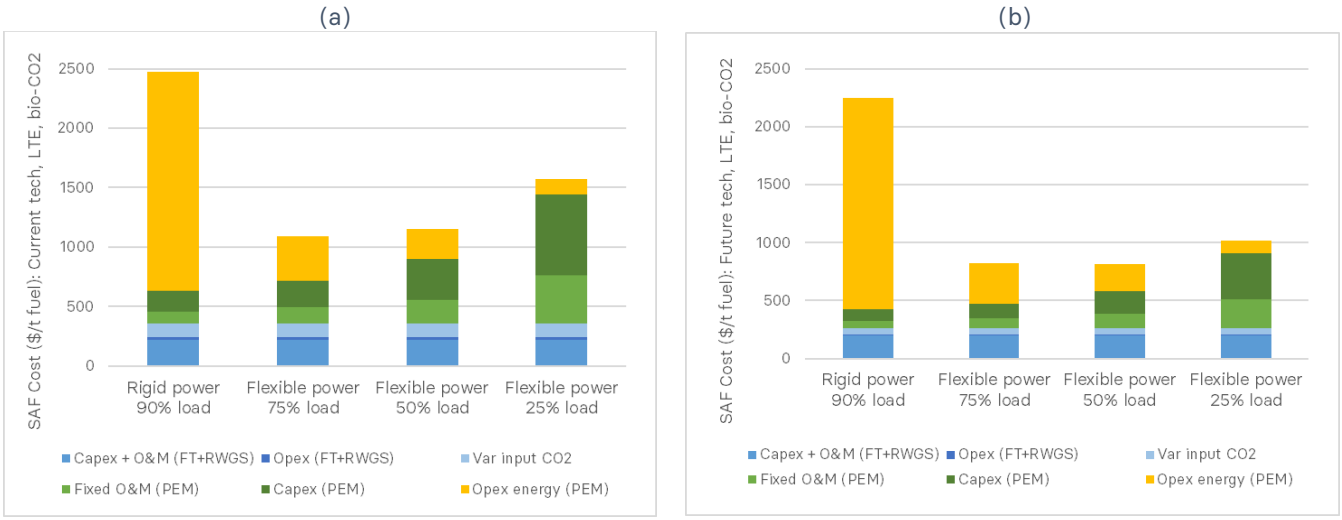

Figure 3. Likewise, the low-temperature PEMEC (PEM) route exhibits significant cost reductions from flexible demand power prices whether using current (a) or future (b) technology efficiencies. The energy feedstock cost share at baseline conditions, 74-81% of fuel cost, is even larger than in the high-temperature route due to the higher stoichiometric H_2 needs for CO_2 activation via RWGS.

Carbon sources can affect expenses by a few hundred dollars per tonne of fuel output (Figure 4). Purchased PSC CO_2 "costs" the e-SAF facility less than DAC, due to ease of capture at higher concentrations. Electric expenses are a main cost driver for DAC as well, and therefore another component where the fuel value chain will see prices tamed as the grid transitions.

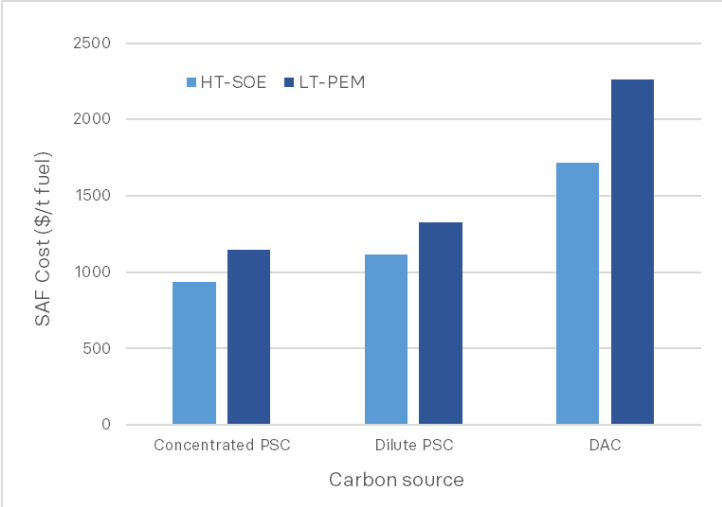

Figure 4. Effect of differing carbon capture sources on total levelized SAF production costs for high- and low-temperature e-SAF routes using renewable power at 50% load, $10/MWh: concentrated (largely biogenic) industrial point source streams, dilute (typically fossil) industrial flue gas, and DAC. Present-day CO_2 prices are around $35/t$CO_2$ for concentrated PSC, $90/t$CO_2$ for dilute PSC, $275/t$CO_2$ (levelized) for high-temperature DAC, and $375/t$CO_2$ (levelized) for low-temperature DAC.

Although the minimum jet fuel selling prices of the e-SAFs may seem out of budget for buyers and refiners, their abatement cost proves competitive (Figures 5, 6). In addition to production cost by mass, we also evaluated and compared emissions reduction cost. Of the current market-mature pathways, HEFA-SPK processed from waste tallow or other waste fats has the most competitive abatement cost at $147 and $69 per tonne CO_2 in 1st and nth plants, respectively. Emissions reduction costs for ATJ pathways are roughly triple that, and gasification-FT pathways six- to sevenfold. As e-SAF pathways operated on surplus electricity achieve nearly 100% carbon emissions savings on a lifecycle basis, the CO_2 abatement performance relative to incumbent pathways reveals advantages not evident from comparing sticker prices by fuel mass. Furthermore, the opportunity cost of *not* pursuing possibilities for a grid-balancing option like PtL would be to stymy innovation in the broader power system transition (IEA, 2021a).

Abatement cost for biogenic and fossil PSC routes in scenarios where the facility is coupled with the renewable power sector lies in the $100-150/t$CO_2$ range. The high-temperature route under certain conditions delivers emissions savings at a price as low as $40/t$CO_2$ now and -$23/t$CO_2$ in the future (the latter implying synthetic SAF cheaper than conventional Jet-A). These abatement costs are competitive with that of the best-performing biomass-based SAF and well within what carbon markets and taxation schemes assign to the price of carbon. Whereas DAC-based e-SAF on rigid baseload demand can be very expensive to operate, abatement costs in our flexible-demand scenarios are tempered by at least half relative to the baseline.

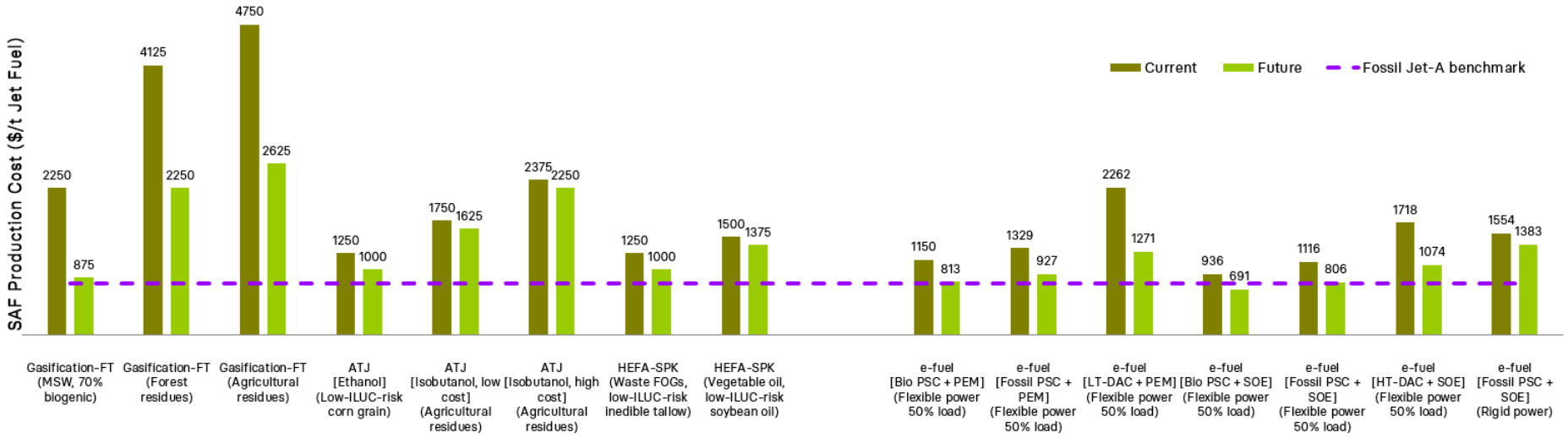

Figure 5. Present and future fuel production costs for biofuels (gasification-to-FT, alcohol-to-jet, hydroprocessed esters and fatty acids [HEFA-SPK]) and e-SAF (low-temperature = PEMEC+RWGS+FT, high-temperature = SOEC+FT) pathways, as compared to a fossil Jet-A benchmark price of $780/t. We assume that any operational pathways fully address health hazards along the value chain, such as particulate matter pollution from crop field tillage, or dioxin formation during gasification of municipal solid waste (MSW). Total PtL production cost varies as a function of the route (high- or low-temperature; carbon source) and utility prices. All e-SAF represented here are produced via electrolytic syngas to FT synthesis.

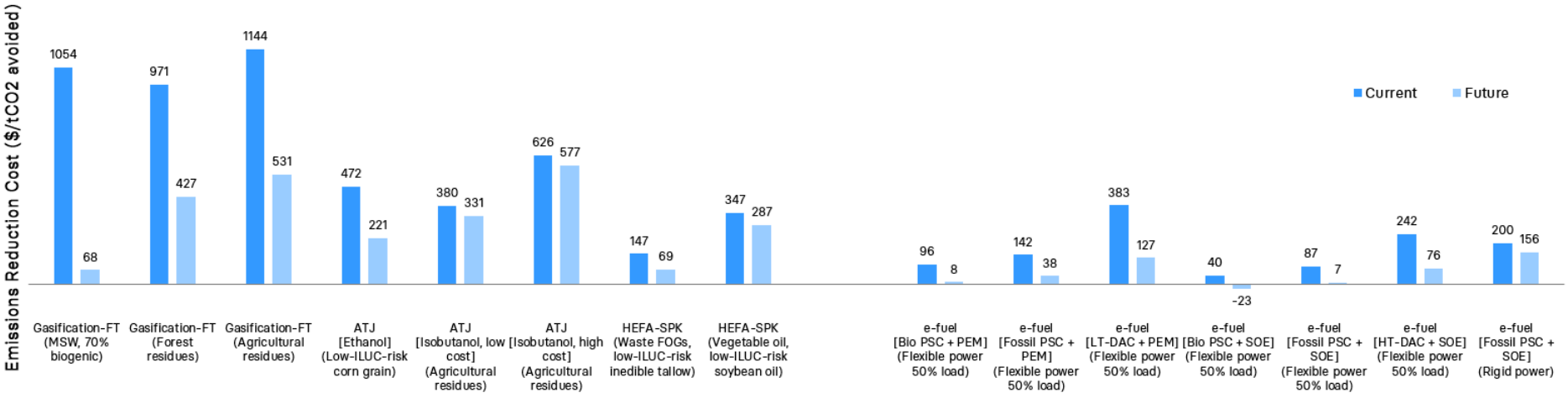

Figure 6. Present and future abatement costs for biofuels (gasification-to-FT, alcohol to jet or ATJ, HEFA-SPK) and e-SAF (low- and high-temperature) pathways, with varying feedstocks and technology choices.

5.1.1. Sensitivity analysis

Sensitivity tests as shown in Figure 7 depict the response of total e-SAF production cost and consequent abatement costs to two main input parameters, electricity prices and CO_2 prices.

Looking at a notional range of grid contract prices for electrolysis on flexible demand, a change of ±5¢/kWh translates into a $592 difference per tonne of e-SAF in the high-temperature route, and $1248/t kerosene in the low-temperature route. The same increase or decrease of 5¢/kWh corresponds to a difference in abatement cost of $153/t$CO_2$e and $322/t$CO_2$e for high- and low-temperature routes. Any change in power price has a greater consequence for the low-temperature route than for the high-temperature route because it has a higher electric need per the H_2 stoichiometric requirement.

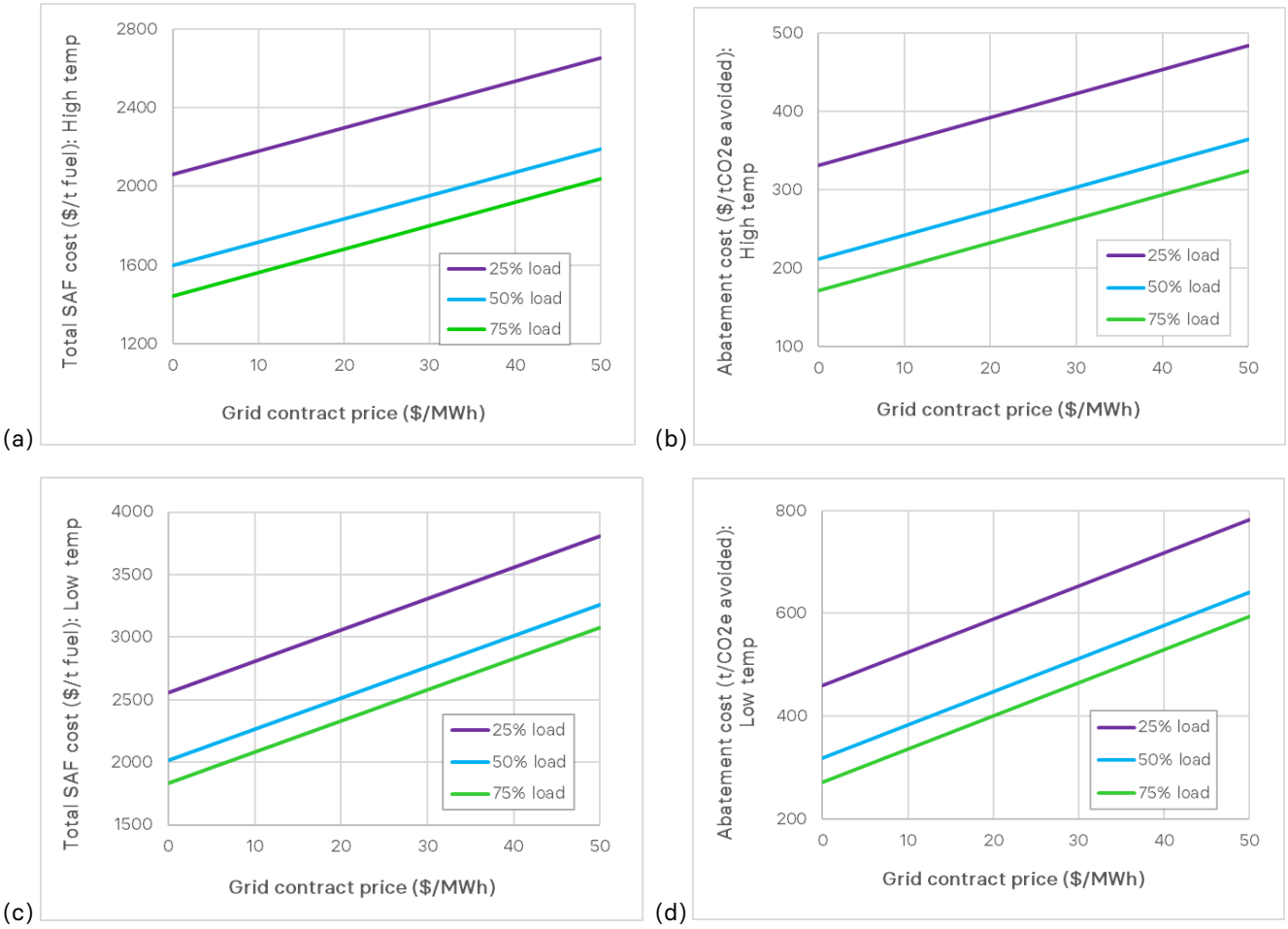

Figure 7. FT e-SAF mass-based cost curves (a), (c) and abatement cost curves (b), (d) at each of 25%, 50%, and 75% load factors in response to power price, for high-temperature (a), (b) and low-temperature (c), (d) routes. (The slope is the electricity demand of the process train). The lower the load factor, the higher the capital costs. Abatement costs are calculated relative to a conventional fossil kerosene baseline of selling price at $780/tonne (Platts, 2024) and lifecycle emissions at 89 gCO_{2e}/MJ (ICAO, 2021), attributing zero carbon intensity as discussed earlier to the surplus units of electricity powering the e-SAF facility. The carbon source is DAC for these plots, and therefore PSC-derived fuels would see the cost curves transposed downward.

5.2. Power grid capacity expansion

The USENSYS grid expansion model optimized the locations and capacities of weather-driven renewable power generation, storage, and PtL technologies over the course of a net-zero by 2050 trajectory, with hourly and regional resolution. Under certain conditions, the option of flexible electrolytic hydrogen production provides mutual benefits to both the power grid decarbonization transition and the growth of e-SAF manufacturing prospects. When the electrolysis operator is willing to buy part-time electricity during hours of excess generation, even at prices an order of magnitude below the average LCOE, this slice of flexible demand allows the grid to avoid wasted capacity. The two-way fuel cell option in particular boosts grid resilience in terms of fulfilling baseload on less installed generation, battery, and storage. This H_2-to-power source also facilitates earlier fossil infrastructure retirement. From the perspective of the e-SAF manufacturer, there is a substantial quantity of cheap power available.

5.2.1. Supply-side capacity structure over time

The USENSYS model reports capacity shares by generation type. In 2030 solar and wind capacities are comparable, with wind at 670-710 GW somewhat greater than solar at 580-630 GW (Figure 8). Further expansion through 2040 to 2050 shows a dominant role for solar generation. By 2040 installed solar reaches 1200-1400 GW, and 2050 capacity in some scenarios approaches 2700 GW. Wind capacity grows more slowly, reaching 870-950 GW by 2040 and 1050 GW by 2050.

The 2050 net-zero policy requires some fossil thermal capacity retirement before the end of its book life (Figure 9). Roughly one-fourth of the initial 142 GW coal-fired generation capacity is forcibly retired in the early years 2023-30; another 41% ages out by 2040, and the remaining 34% winds down by 2050. Natural gas-fired generation sees a more delayed phase-out in REF_ZERO and the one-way PtL scenarios. About 20% of the initial 456 GW capacity is retired in 2030, then 4% by 2040 and 60% in the last decade to 2050. Some 16% of the initial capacity reaches the end of its book life at various timepoints.

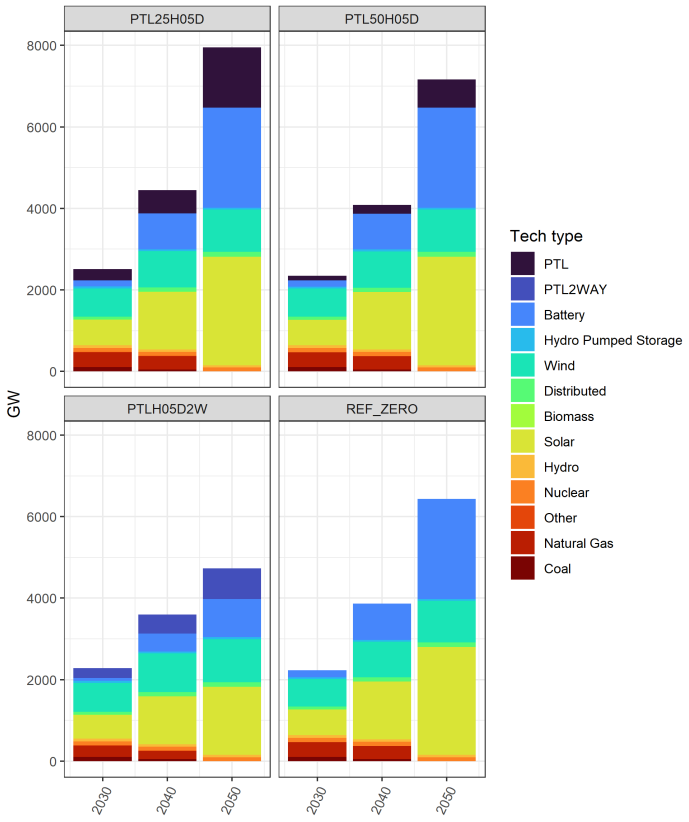

Figure 8. Installed generation and storage capacity by technology type.

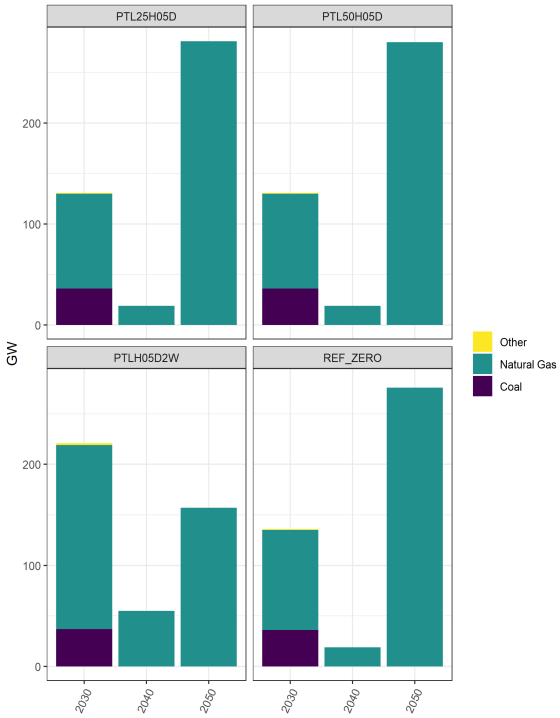

Figure 9. Early (cost-induced) retirement of pre-existing fossil thermal generation capacity

5.2.2. Demand-side capacity structure over time

All the scenarios take the same baseload demand trajectory over time. Variations in total GWh generated are driven by each scenario's levels of flexible PtL activity, or in other words, watt-hours that might have been curtailed but were instead generated and consumed in real time by the electrolyzer.

Real-time consumption for electrolysis, pumped hydro storage, and battery storage compete for surplus based on least cost. Battery storage takes the lion's share of installed capacity (GW) and usage (GWh) from 2040 onwards, in REF_ZERO and the one-way PtL scenarios. Beginning from 150-170 GW in 2030, battery capacity grows more than fivefold to 2040 and nearly triples again the following decade.

Table 4 summarizes national generation capacity, demand, PtL capacity, and curtailment over the three decades. The baseload is consistent across scenarios. Introducing the PtL options allow the grid to generate more and curtail less compared to the reference case. Notably, the PtL options reduce curtailment by at least an order of magnitude, and even two orders under certain load and year conditions. After 2030, the scenario using electrolysis at a 50% load threshold provides the highest generation capacity among the modeled scenarios.

Table 4. Summary of capacity structure over time. Estimates represent nationwide totals.

	Year	REF_ZERO	PTL25H05D	PTL50H05D	PTLH05D2W
Baseload (TWh)	2030	4518	4518	4518	4518
	2040	5916	5916	5916	5916
	2050	6964	6964	6964	6964
Generation (TWh)	2030	5321	5418	5464	5568
	2040	8055	8200	8254	8095
	2050	11559	11778	12333	10100
Curtailment (TWh)	2030	536	56	223	81
	2040	1192	62	388	131
	2050	3038	4	103	70
P2L input (TWh)	2030	NA	603	473	788
	2040	NA	1257	939	1442
	2050	NA	3236	3018	2012
Reverse fuel cell output (TWh)	2030	NA	NA	NA	67
	2040	NA	NA	NA	209
	2050	NA	NA	NA	406

5.2.3. Effect of flexible PtL on power sector resilience

Without PtL integration, the only DSM options are battery and pumped hydro storage. Adding PtL to diversify the basket of demand sinks results in higher installed VRE generation capacity compared to the reference net-zero case. Most of the surplus goes to H_2-PtL without affecting the battery capacity.

PtL operating hours are most concentrated during the summer months (Figure 10). This is especially helpful to power systems with an increasingly winter-peaking demand profile in a natural world where the sun continues to shine most during summer. Over the course of each day, PtL operation is highest around solar noon, a few hours earlier than peak demand.

Inter-regional transmission capacity is relatively uniform across scenarios. There are modest expansions over the three decades, attributable to just 8 of the 49 regional interconnections, and most take place during the 2040-50 decade. New-build transmission lines are relatively expensive compared to the other options in this model. Storage is also more spatially suitable for the dominant share of solar generation, as PV sites tend to be located closer to industrial centers and does not need as much long-distance transport as wind power.

Total curtailment is dramatically improved in the PtL scenarios relative to the reference net-zero case (Table 5). Absent PtL whatsoever, the power sector has few tools to contend with variability, leaving 3 million GWh of consumable generation untapped (Figure 11). In the reference case, the Upper Mississippi, New England, Great Basin, and north-central Appalachia show particularly large mismatches between consumption and generation (Figure 12).

With PtL, the leftover watt-hours are used by electrolyzers at their moment of generation instead of being curtailed. This slashes “wasted” or “lost” capacity by at least two-thirds and up to 95% in 2040. Curtailment in the PtL scenarios is effectively eliminated by 2050.

Table 5. Curtailed MWh per generated GWh

Year	REF_ZERO	PTL25H05D	PTL50H05D	PTLH05D2W
2030	104.3	10.7	42.1	14.8
2040	163.4	8.4	52.2	17.2
2050	295.4	0.4	9.8	7.6

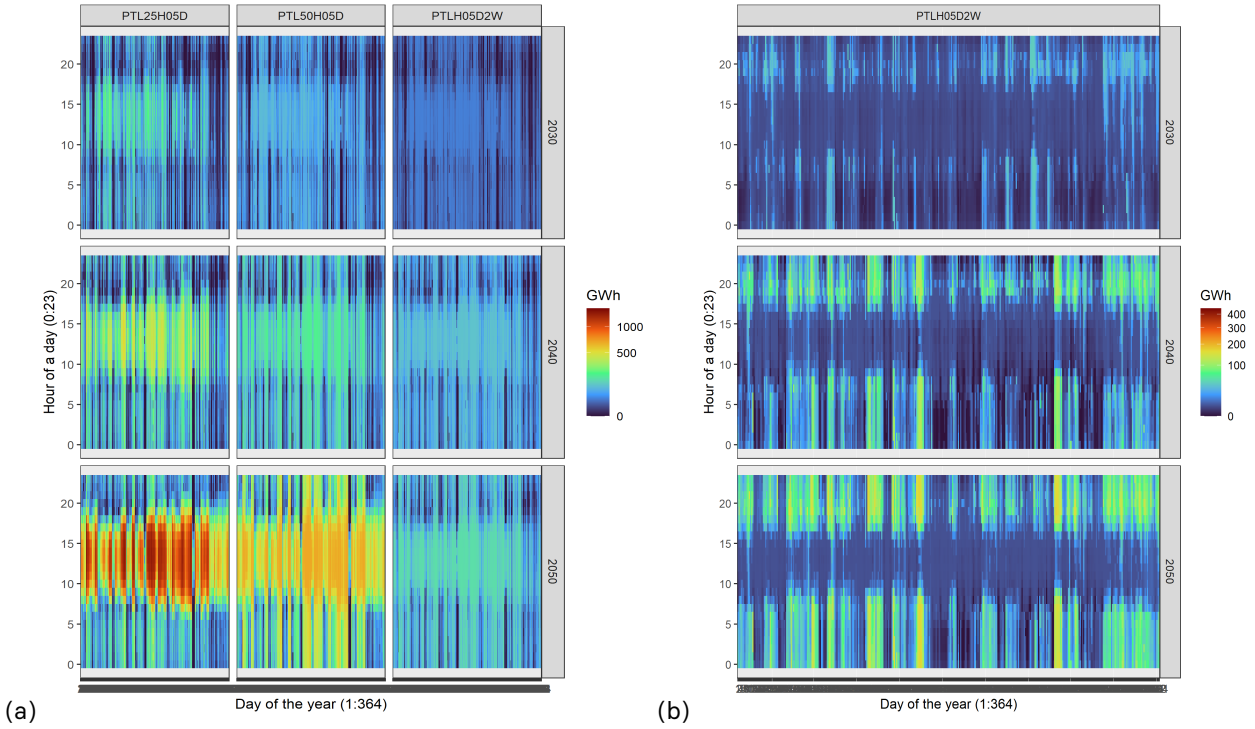

Figure 10. Nationwide energy input (GWh) to (a) electrolyzers as electricity and (b) fuel cells as hydrogen, daily over the course of the year.

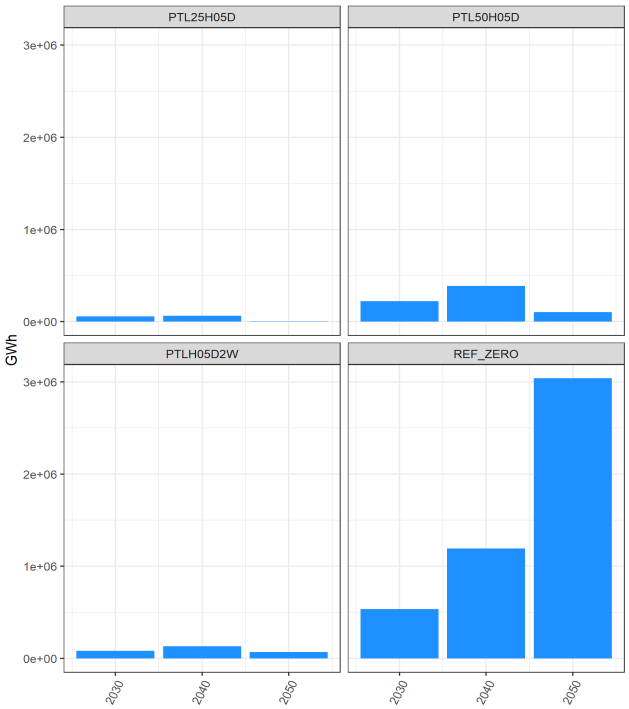

Figure 11. Total curtailed energy by scenario, over three decades.

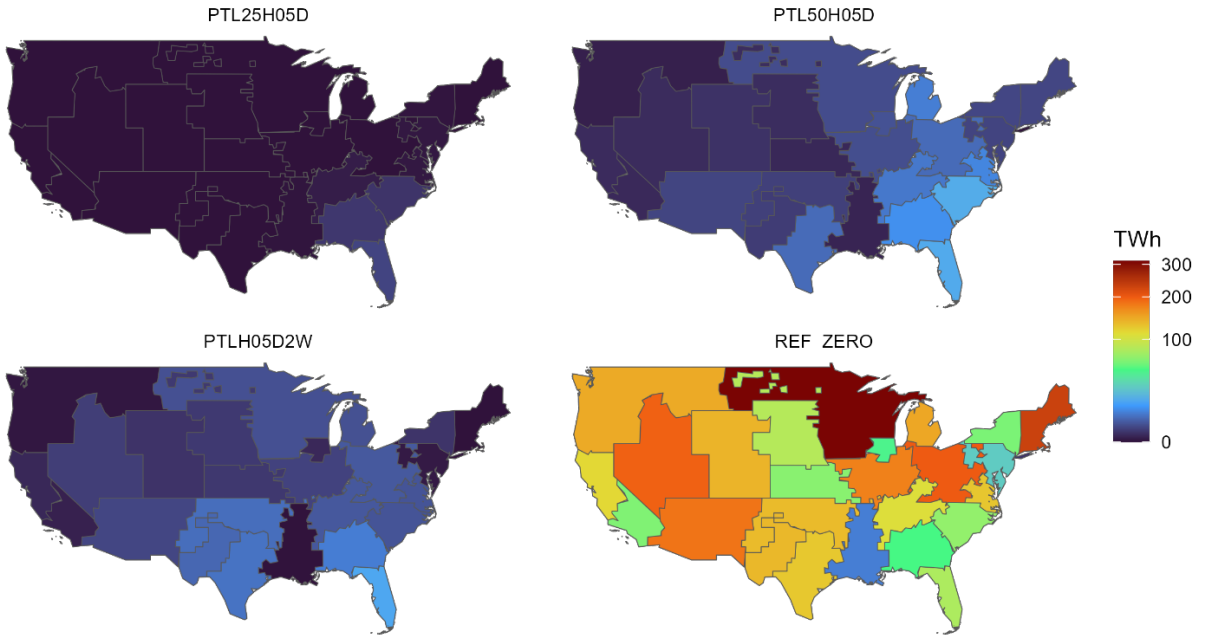

(a)

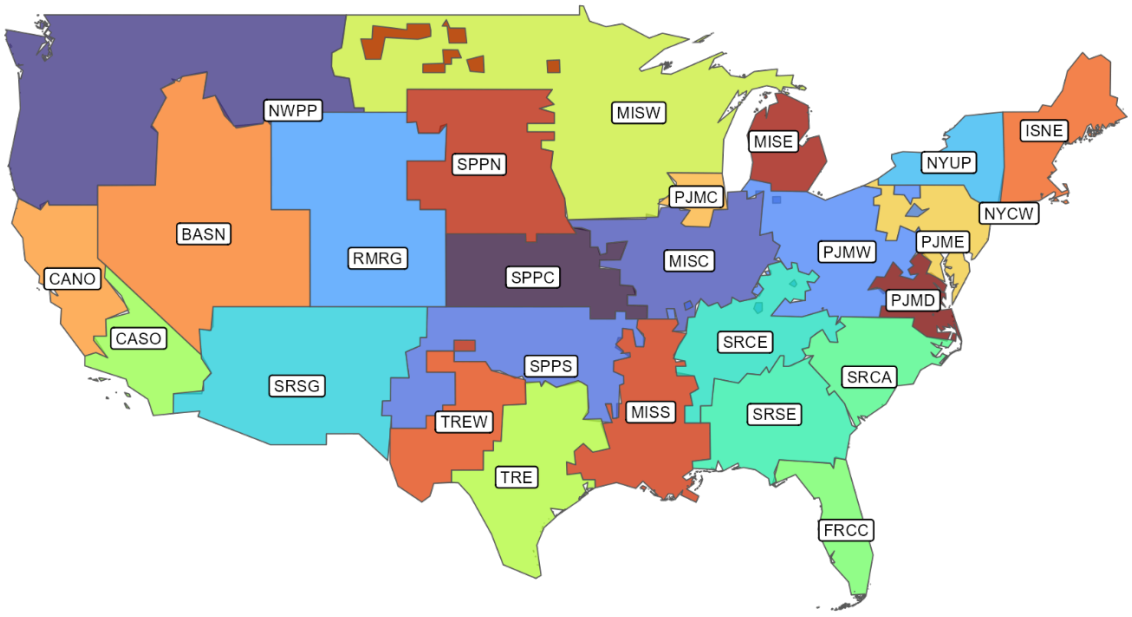

(b)

Figure 12. (a) Annual curtailed generation (TWh) in each grid region at year 2050. Region names are depicted in (b), with generic colors.

5.2.4. Effect of bi-directional PtL and fuel cells on power sector resilience

Bi-directional hydrogen/power production offers a back-up power source and thus streamlines grid efficiency in terms of infrastructure needs. PTLH05D2W needs only half as much battery capacity as the other scenarios in the first decade. As the load factor of battery charging evolves over time, the gap in GWh capacity widens to the point where this scenario with two-way electrolysis involves only ¼ as much battery activity as the other scenarios (Figure 13).

Whereas one-way PtL made little difference in transmission compared to the reference case, the two-way settings do deliver transmission savings: the total capacity is nearly static, seeing less than 5% change between 2030 and 2050 (Figure 14).

Natural gas retirement is front-loaded in the early years instead of delayed until the 2041-2050 decade (Figure 9 above). Forty percent of the initial 456 GW capacity is decommissioned by 2030, another 12% by 2040, and the remaining 34% retired in the last decade.

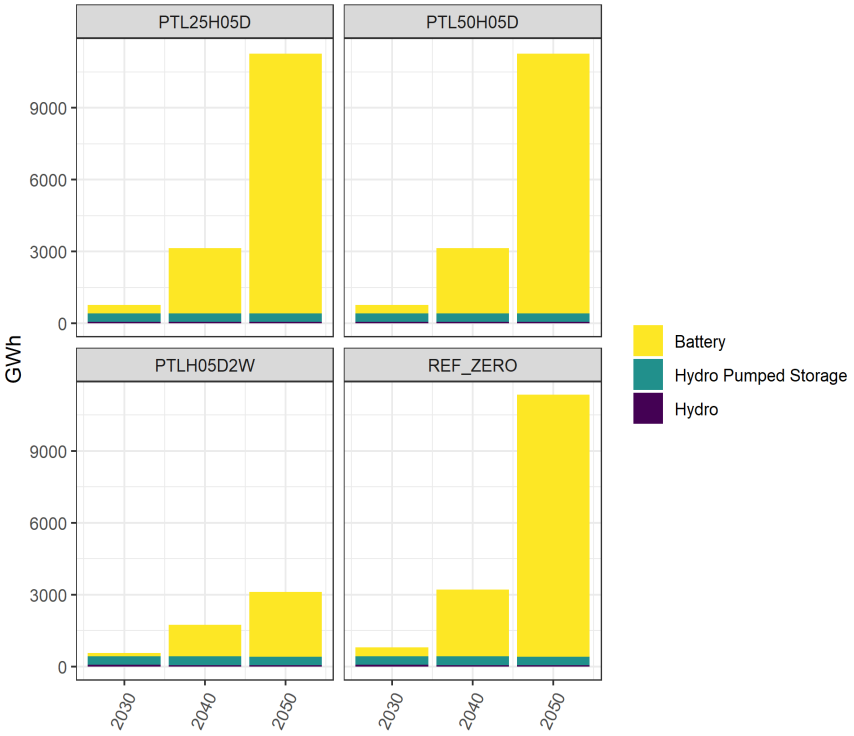

Figure 13. Energy (GWh/yr) sent to battery, pumped hydro, and hydropower storage.

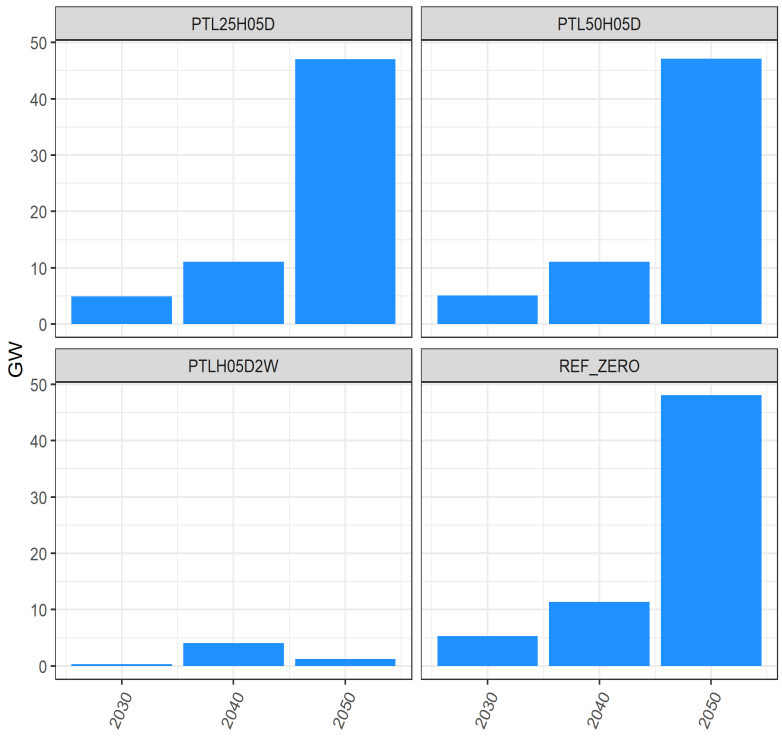

(a)

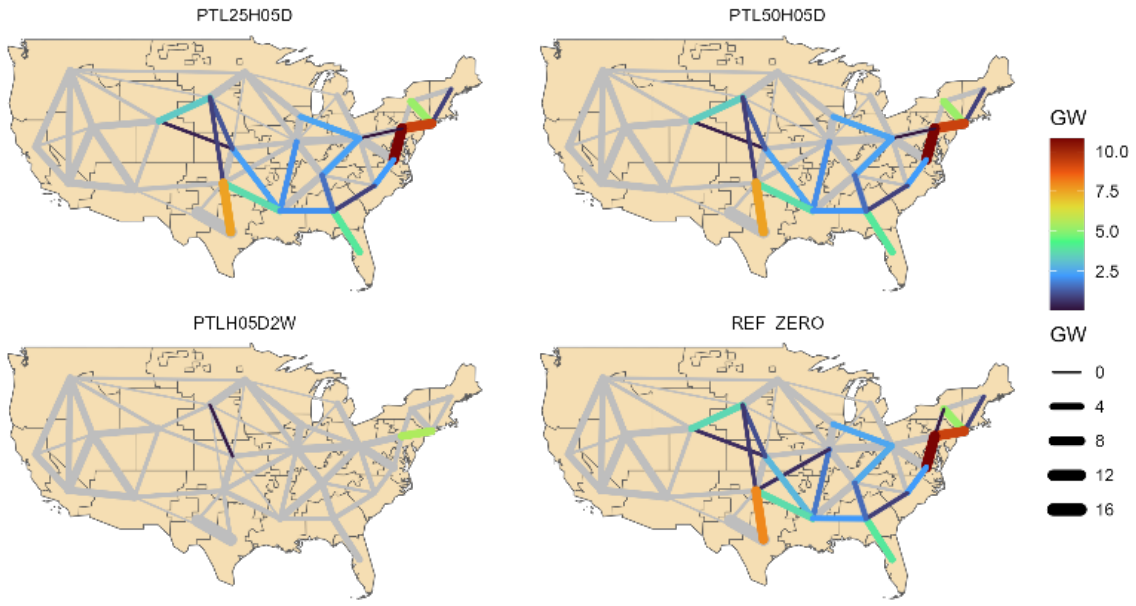

(b)

Figure 14. Transmission expansion displayed as (a) nationwide total over decadal progression and (b) cumulative capacity increase over 2023-2050 for each interregional connection

5.2.5. Power-to-liquid operation: Surplus potential for hydrogen-based fuel

The siting of PtL technologies varies by region and is dependent on the local interaction between supply and demand. Regions with high potential H_2 output include MISW, TRE, ISNE, BASN, and NWPP, which stand for Upper Mississippi Valley, Texas, New England, Great Basin, and Northwest, respectively (Figure 15). In practice, working H_2 capacities will also be contingent on freshwater availability, either naturally occurring or desalinated from ocean sources.

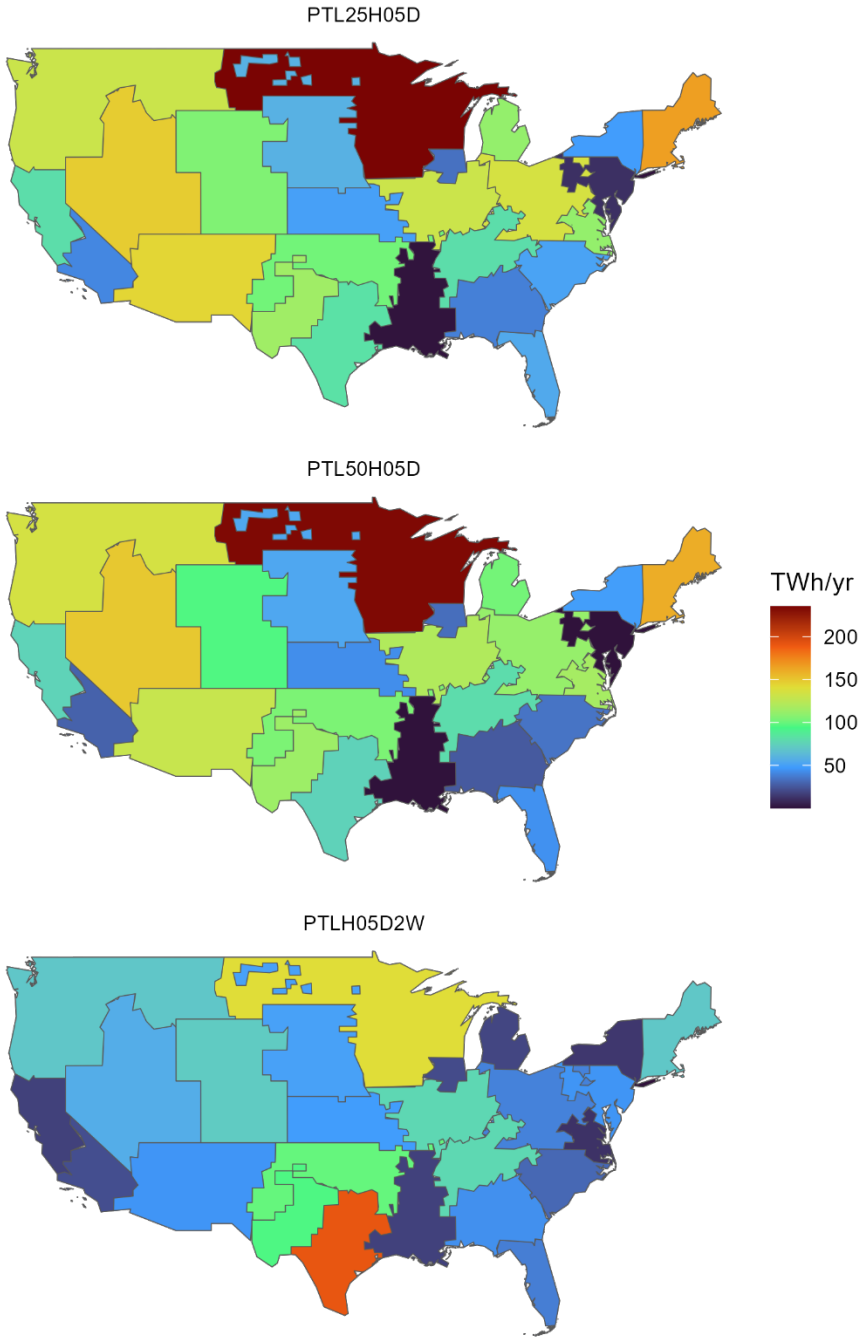

Figure 15. Annual H_2 output (TWh/yr) by region in year 2050, before fuel cell consumption

Jet fuel demand in the U.S. in 2050 is expected to be 35 billion gallons (SAF Grand Challenge, 2021), which is equivalent to approximately 1385 TWh of energy content. The estimated surplus energy allocated to hydrogen production in the U.S. in 2050 is 2012-3236 TWh. At an electrolytic energy efficiency of approximately 70%, this is sufficient to produce 1409-2265 TWh of hydrogen output (Table 6), all scenarios greater than the expected 1385 TWh of sectoral demand. For e-SAF routes using waste CO_2, there is a modest energy consumption for the remaining steps, but the electrolytic step still represents the bulk of the energy requirements. For a DAC-to-PtL route fully running on renewable power, the overall caloric efficiency is around 35-50%, in which case a national power surplus of 3236 TWh translates to finished e-SAF satisfying at least four-fifths of, and possibly surpassing, sectoral demand. At decadal waypoints, the electrolytic output reaches 331-551 TWh in 2030, and 657-1009 TWh in 2040.

Table 6. Hydrogen production and self-consumption (GWh). Negative values indicate energy returned to the grid as electricity. H_2 production values represent 70% of the original grid electricity received. For the two-way scenario PTLH05D2W, net hydrogen sales are the sum of the values in the two columns.

Scenario	Year	H_2 production	H_2 self-consumption
PTL25H05D	2030	421,900	N/A
PTL25H05D	2040	879,649	N/A
PTL25H05D	2050	2,265,142	N/A
PTL50H05D	2030	331,222	N/A
PTL50H05D	2040	657,006	N/A
PTL50H05D	2050	2,112,711	N/A
PTLH05D2W	2030	551,733	-95,810
PTLH05D2W	2040	1,009,559	-298,593
PTLH05D2W	2050	1,408,505	-579,685

By 2030, the Midwest has potential to supply 4.6 million tonnes of hydrogen, of which Minnesota, Iowa, and Wisconsin (Upper Mississippi Valley, MISW) account for half, and Illinois, Indiana and Missouri (Middle Mississippi Valley, MISC) another quarter. Paired with the 46 million tonnes of high-purity waste CO_2 from existing industrial ethanol fermentation (EIA, 2023; Dees, 2023; USDA, 2024), this green H_2 becomes 9.7 to 13.4 million tonnes of clean e-SAF, or 3.2 to 4.4 billion gallons (Table 7). In other words, e-SAF synthesized in the Midwest alone could deliver a bulk of the 2030 national SAF Grand Challenge target of 3 billion gallons. Replacing this volume of conventional jet fuel with synthetic e-SAF at a near-zero CI also scores lifecycle emissions savings equivalent to about one-seventh of the total national 292 million tCO_2e of commercial aviation emissions in 2019, as estimated by the Federal Aviation Administration (FAA, 2021). Furthermore, this e-SAF made from concentrated PSC CO_2 is projected to have the lowest production cost (Figure 4).

By 2040, e-SAF potential in the Midwest reaches 11.1 to 16.9 million tonnes, or 3.7 to 5.6 billion gallons. As the Corn Belt creeps northward amid warmer seasons, its geographic center will also converge upon

MISW where wind power is plentiful. Minnesota and the Dakotas are likely to evolve from being the border of the Corn Belt to seeing full season production (Hoffman et al, 2020).

Table 7. Potential 2030 capacity of syngas inputs (million tonnes, *Mt*) and e-SAF product (million gallons per year, *mgy*) in the US Midwest in the two-way scenario PTLH05D2W. The lower bound e-SAF output is estimated from the low-temperature route given its larger H_2 mass requirement.

a: derived from grain ethanol production data in (EIA, 2023), (Dees, 2023), (USDA, 2024)
b: in SPPC, free CO_2 is the limiting reactant rather than electrolytic H_2

Region	Net H_2 to SAF (Mt)	Fermentation CO_2 (Mt) [a]	e-SAF volume, lower bound (mgy)
MISW: upper Miss. Valley (*Wisconsin, Minnesota, Iowa*)	1.95	19.1	1465
MISC: middle Miss. Valley (*Illinois, parts of Indiana and Missouri*)	1.04	7.5	784
SPPN: northern Great Plains (*North Dakota, South Dakota, Nebraska*)	0.69	12.1	520
PJMW: Ohio Valley (*West Virginia, Ohio, part of Indiana*)	0.17	4.0	125
SPPC: central Great Plains (*Kansas, part of Missouri*)	0.64	2.2	226 [b]
MISE: Michigan	0.08	1.0	58
Total Midwest	**4.57**	**45.9**	**3178**

Aside from two-way electrolyzer modes, the other key characteristic of the PTLH05D2W scenario is that intermittent electricity is made available to buyers at three load levels, each with its own price. This helps the model capture a spectrum of users, which is more realistic in the market than a single load factor threshold. Total hydrogen production in the two-way scenario, before fuel cell consumption, starts out more active than either the PTL25 or PTL50 setting alone in the early years; then, by 2050, electrolysis in the PTL25 and PTL50 settings surpasses PTLH05D2W. This mirrors the patterns in generation expansion over time: where a smaller installed capacity can satisfy the national baseload, fewer surplus watt-hours need to be dealt with.

Even so, the electrolyzers in 2050 receive 914 TWh of electricity at 75% load or higher, out of a total of 2012 TWh across the three load-price levels. The reverse fuel cell mode becomes more involved over time: in 2030 this process consumes 17% of produced hydrogen, in 2040 it uses 30%, and in 2050 the share grows to 41% self-consumption (Table 6). Assuming 70% fuel cell efficiency, this 580 TWh in 2050 translates to 406 TWh of backup electricity ready at the flip of a switch. Fuel cells are most active in Long Island's grid region, followed by the Gulf Coast and New Jersey (Figure 16).

The results of this modelling prove the study concept that hydrogen production can provide a critical demand-side flexibility option that helps to balance the grid. As notably demonstrated in scenario PTLH05D2W, there are significant decreases in battery storage, new-build transmission, and curtailment upon the introduction of two-way electrolysis.

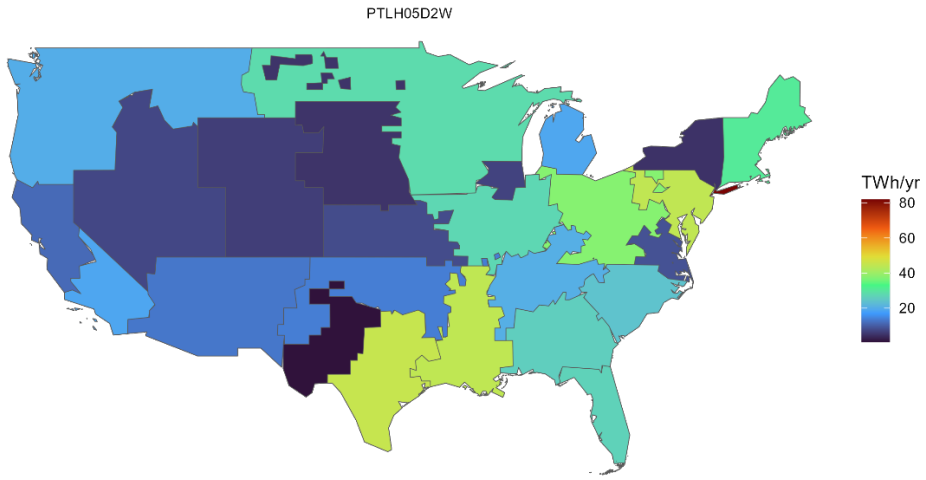

Figure 16. Fuel cell consumption of H_2 (TWh/yr) in the two-way electrolysis scenario, by region in year 2050.

The results also prove the overall concept that there will be sufficient surplus renewable electricity to support fuel production for aviation. Although the surplus electricity will ultimately be shared among various flexible-demand end uses, competition for spare energy is likely to be tempered by a growing understanding that priority among end uses should be reserved for those for which the fundamental laws of physics present the greatest barriers to electrification, i.e. prioritizing long-haul air and marine transport.

6. Caveats

This section provides a comprehensive analysis of the caveats associated with system definition, cost uncertainties, and carbon intensity. These factors play a crucial role in shaping the outcomes and interpretations of our results. This section aims to offer a clearer understanding of their potential impact on our findings and conclusions.

6.1. System definition

6.1.1. Power source

Our USENSYS modeling assumed a particular set of future what-if conditions around policy and investment decisions, and therefore it portrays only a subset of possible grid configurations.

If greater demand across sectors arises than that forecast in PowerGenome, additional generation capacity will be required to accommodate peak usage. These generation maxima will result in additional surplus electricity available on a national aggregate level beyond what our model estimated, even after meeting the elevated baseload shares already spoken for by household & other industrial usage. The IEA estimates baseload demand in 2050 to be 40% to 50% higher than today (IEA, 2021a).

On the other hand, if other DSM strategies not represented in our model come into widespread use, then less electricity will be directed toward PtL than what we predicted. Many of the excess watt-hours generated around solar noon were sent to PtL simply because that is the most cost-effective option at those moments in those locations, given what was offered in the model. Had more load-shifting measures been represented in the model – such as inexpensive short-duration storage, heavy duty

electric vehicle charging, or expansion of green hydrogen use in industrial chemicals manufacturing -- a substantial share of watt-hours may have been diverted there instead of sent to hydrogen production. Furthermore, major incentives such as the US 45V hydrogen production tax credit could expand demand for the same quantity of surplus watt-hours, and/or conversely stimulate additional VRE generation capacity. Thus, contextual factors outside what our model captures could push the volume of surplus electricity for aviation either higher or lower than the estimates presented here.

Furthermore, the model's endogenous interactions between flexible PtL activity and the grid are based on energy requirements for hydrogen production, rather than energy for the complete fuel production pathway. That said, electrolysis is the most energy intensive step in the process train, meaning that the hydrogen production component provides an order-of-magnitude indication of total energy demand. Our USENSYS runs use hydrogen production as a simplified representation for e-SAF facilities' interaction with the grid, to put emphasis on assessing the general concept of bi-directional grid balancing potential. Conceptually, the electrolyzer-fuel cell could be replaced by an agnostic flexible two-way technology, and the rest of the study design would remain the same.

For fuel manufacturing, we assume that the power source is grid-connected and restricted to surplus watt-hours. Standalone hybrid PV-wind generation for the e-SAF facility is an alternate possibility in locations that can bear both the capital and carbon costs of equipment construction. For instance, in regions with plentiful PV and wind potential, VRE can deliver renewable power at nearly full-time capacity, thus enabling both optimal capital expenditures and semi-dynamic operation on low-cost power supply. Such an arrangement brings LCOD down to 70–80 €/tCO_2 by 2040 and 55 €/tCO_2 by 2050 (Breyer et al., 2020), assuming VRE carries negligible embodied emissions.

6.1.2. Fuel plant configuration

When assigning input energy demand in our model, the choice was made to electrify wherever possible to minimize fossil input (typically by replacing natural-gas-oxyfired heating with electric heating). This provides a high-bound estimate of electric demand. The heat transfer calculation is subject to the boundary condition that recycled FT heat is less than DAC thermal demand, as electrical energy can be converted to resistive thermal reasonably efficiently, but not vice versa. Although high-temperature electric kilns like the ones needed for HT-SOEC and HT-DAC are currently limited to specialized industrial applications, there is sufficient demand for the technology such that widespread industrial adoption of electrified heating is not far away (Sherwin, 2021).

The thermal coupling configurations in our model take one heat sink for each configuration and assume that waste heat is recovered by means of heat exchangers, transferring always from higher to lower temperature. However, depending on optimization of individual plant equipment, heat pumps may prove useful in upgrading and channeling low- and medium-grade waste heat to higher-temperature modules in the process train such as a 900°C calciner - especially as improvements in heat pump technology facilitate recovery ratios greater than current performance.

Furthermore, engineers may choose to split up source heat to multiple sinks within the process train. For instance, within the low-temperature route, part of the thermal energy could be sent to the RWGS reactor operating at 600°-800°C, rather than all to the DAC module. Likewise, other efficiencies can be

employed in the basic heat exchange technology; heat emanating from an FT reactor at 300°C can be used to boil water or preheat inlet gases to a LT-DAC unit or the electrolyzer stacks.

6.1.2. Geographic co-location of inputs

Inputs to the e-SAF value chain need to be brought from their respective points of generation, production, or capture to a common location for FT synthesis. There are multiple ways to transport electricity, water, and CO_2, and thus we assume production engineers have optimized the logistics. For instance, electrolyzers and FT reactors could be clustered at existing sites of industrial fermentation in Illinois, powered by wind farms in Missouri, and the estimated total e-SAF availability for the grid region MISC assumes sufficient intra-region transmission across MISC. In general, we observe that e-SAF synthesis at the site of carbon capture is likely to be preferable given the safety and health risks that new CO_2 transport pipelines would pose to landscapes and communities. On a similar note, the potential for H_2 pipeline leaks and their sizeable warming potential (Esquivel-Elizondo et al., 2023) warrant consideration of sending electrons through cables to *in situ* electrolyzers, rather than attempting to transport finished hydrogen.

6.2. Cost uncertainties

6.2.1. Power prices

Grid contract pricing was assumed at a handful of plausible price points for each level of capacity utilization. In reality, the landscape of contract prices is highly heterogenous and not always underpinned by physics. Whereas our model's aim was to illustrate the concept of a flexible power system's benefits vis-à-vis a rigid power system - with less emphasis on the exact power prices - more granular analyses of the load-price dynamics and consequent effects on minimum jet fuel selling prices are the focus of other groups' research (Adelung, 2022; Malins, 2017; Grahn et al., 2022). Even despite the uncertainties, e-SAF cost reduction should progress more quickly than quoted in mainstream literature. Those assessment models tend to rely on assumptions that overestimate the present and future electricity cost burden (Breyer et al., 2019).

6.2.2. Capex

Future capital costs are highly responsive to technological learning rates, which are difficult to predict without knowing the conditions imposed by future public and private investment decisions. For example, the Hydrogen Production Tax Credit in the Inflation Reduction Act could jumpstart the learning curve for water electrolysis and enable rapid capex reductions during the credit's short but opportune window of applicability.

The earlier in its development trajectory a technology is, the greater the uncertainty in cost estimates (Rojas-Michaga et al., 2023). In the case of DAC, capex figures span two orders of magnitude from ~\$60/tCO_2 to ~\$3000/tCO_2. Despite these wide ranges, the industry target of \$100/tCO_2 is grounded in realistic physics and will be closer in reach when large-scale n^{th}-of-a-kind DAC plants come online (NASEM, 2019; Sabatino, et al., 2021). IEA's projected net zero trajectory involves global CO_2 capture totals increasing to 1.6Gt/year by 2030 and 7.6Gt/year by 2050 (IEA, 2021a). If responsible and forward-looking policy planning fosters rapid technological learning of modular PtL technologies as it

has for solar PV, then DAC and PtL could prove accessible and cost-effective sooner than predicted by mainstream discussions (Breyer et al., 2019).

Certain physical characteristics are tough to generalize across installments but can be predicted from current knowledge. For instance, electrolyzer stack replacement frequency depends on the degradation rate from cycling the electrolyzer on and off per supply fluctuations, particularly for SOEC with its wide magnitude of thermal cycling. Therefore, locations with more frequent oscillations in their daily power profile would likely experience faster stack degradation and therefore greater accumulated replacement costs over the plant lifetime. Fortunately, variable current density does not affect the tuned syngas H_2:CO ratio (Dittrich, et al., 2019).

6.2.3. H_2 storage to facilitate steady-state FT synthesis

When electrolysis output is variable but FT synthesis runs at constant load, the time mismatch may require an H_2 buffer. The hourly H_2 storage capacity needed can be calibrated to an individual plant's VRE profile at varying full-load-hour scenarios, as in Fasihi et al. (2016) to provide steady-state feeds for the FT unit. Rather than explicitly assigning an H_2 buffer quantity in our study at each capacity factor, we leave this additional capex assessment to more granular, site-specific studies.

6.2.4. Dynamic operation of the entire process train

Although the majority of FT synthesis and CO_2 activation processes are designed, operated and analyzed at steady state – with H_2 storage options built into fuel production chains to accommodate fluctuating supply – intermittent and dynamic FT modes are also feasible. Dynamic reactor operation may not be as detrimental to reactor reliability as commonly thought, and pulsing of the hydrogen feed may even confer benefits via process intensification and operating windows to drain the reactor bed (Wentrup et al., 2022). The ramping of startup and shutdown is expected to incur an energy penalty on the order of 1 kWh H_2 per Δ1 kW fuel output rate (Sherwin, 2021). In such a configuration, the FT step could both synchronize with H2 output and receive cheaper power prices.

6.2.5. DAC in a VRE-powered world

Our model assumes DAC operates at steady state and pays the LCOE of $50/MWh. The power demand from DAC is nontrivial, at around 8 MWh/t fuel. Under present-day grid conditions at constant load, this raises a concern of either straining new renewables capacity or raising emissions from current fossil generation. However, in the near term e-fuels will rely more on industrial waste PSC than on DAC. By the time industrial fossil flue carbon supply dwindles and biogenic streams are occupied, clean electricity will have expanded substantially, most likely enough to fully satisfy DAC-to-fuel power demand at affordable prices and without inducing any resource shuffling. For grid-connected installations, the LCOE and utility rates will be cheaper than in the present decade. For standalone installations with on-site generation, there will be greater supply of PV and wind equipment, enabling DAC operators to acquire infrastructure without competing against grid needs.

6.2.6. Comparative abatement cost

Abatement cost is a function of all the above factors *plus* the baseline reference fossil jet cost. Jet-A spot prices fluctuate on the order of tens to hundreds of dollars per tonne; the $780/t Jet-A cited here tends

to be a mid-lower estimate (thus giving a conservative estimate of the monetary cost of emissions reduction conferred by SAF). When conventional Jet-A prices push $900-1000 as in 2022, the "green premium" is narrower and therefore users pay less per unit CO_2 avoided (Platts, 2024).

6.2.7. Novel technologies

Companies such as Twelve, Norsk, and Zero Petroleum have full FT e-SAF pilot facilities in operation. Promising research, development and demonstration is also underway on alternative e-SAF production routes that could improve efficiency and significantly reduce costs, including: reaction routes (other than SOEC) for direct electrochemical reduction of CO_2 to CO (Chen et al., 2018); PEM co-electrolysis of CO_2 and H_2O at low temperatures (Kuhl, 2021), and solar thermochemical "sun-to-fuel" reduction (Treyer, 2022). (Synhelion replaces electrolysis and RWGS with a different set of redox reactions, driven by concentrated solar power, to generate the syngas for FT fuels.) There is even a direct hydrogenation route that combines reduction and synthesis in a single reactor (Sheehan et al., 2022).

Furthermore, the technologies discussed are not exclusively bound to their usual temperature ranges; PEM can operate at high temperatures and SOE can operate at low temperatures with certain adjustments. Likewise, solvent DAC can operate in low-temperature regimes and solid sorbent DAC in high-temperature regimes with tuning of the sorption/desorption chemistry (NASEM, 2019). DAC technologies other than the two used in our study include metal-organic frameworks such as Airthena's, (Sadiq et al., 2020), electro-swing adsorption such as Verdox's (Stauffer, 2020), moisture-swing adsorption (Mechanical Tree), and cryogenic (McQueen, 2021).

6.3. Carbon intensity

Our calculations place the energy intensity of the full jet e-fuel pathway at 13-33 MWh/t fuel, or 1.1-2.8 MJ electric input per MJ fuel output. When powered on the current baseload grid mix in most geographies, the e-fuel production cycle itself may have a high carbon intensity – thus unsustainable and counter to its own intent.

It is crucial that the electricity derives from renewable origins and that it does not displace essential baseload uses such as household and healthcare facilities' consumption. Otherwise, jet e-fuels could end up with higher life-cycle emissions – total emissions from production to combustion – than conventional jet fuel. As current electricity grids are at varying stages of decarbonization, securing sufficient renewable energy supply for e-SAF may appear an infeasible task.

One way to ensure the environmental integrity of e-fuels on a life-cycle basis is to rely solely on surplus renewable electricity. Although the equipment in renewables installations does carry a nonzero emissions cost from cradle to grave, in this grid-balancing context the power sector has already borne the responsibility for those attributed emissions (also known as embodied emissions) regardless of whether or not the e-SAF production activity is online to absorb the surplus electricity. In other words, the turbine and PV panel manufacturing emissions lie outside the attributional system bound of the e-SAF in this study. This is in fact consistent with accounting for other fuel types, which do not carry the "emissions burden" of equipment cradle-to-grave lifespan. Furthermore, the e-SAF production induces no new land use footprint additional to the surface area already occupied for grid purposes.

Therefore, barriers to transformation of the power sector and the fuels manufacturing sector must be addressed from the point of view of an integrated system, all while taking care to minimize displacement effects. As we have shown in this proof of concept, the potential for dynamic operation powered by excess renewables indicates promising avenues for ramping up e-SAF production in tandem with successful grid decarbonization.

Interestingly, high-integrity e-SAF could be achieved in some regions using cost-effective surplus renewable power from the grid even when fossil-based electricity is part of the national energy mix. Of course, this works only in a scenario where the country is transitioning to a renewables-based power generation system and has attained a critical level of renewable electricity deployment. Where that is the case, the potential synergies have a materially relevant magnitude. For example, a feasibility study of China's power sector transformation into a renewables-based system found the amount of surplus electricity usable for interruptible demand could in theory power sufficient e-SAF volumes to cover around 10% of global aviation jet fuel demand in 2030 and 100% by 2050 (Lugovoy et al., 2021).

Because reliance on surplus energy de facto constrains siting options to certain locations with abundant renewables potential, several integrated models assess net abatement performance in "competition" with CCS-balanced conventional fossil kerosene usage (Beccatini et al., 2021). Although GHG and dollar cost numbers may appear to favor CCS paired with conventional jet fuel under present conditions, we do not consider continued fossil dependence a "sustainable" course of action. A research team in Leipzig ran an optimization model for Germany's national scope and found that when e-SAF production is operated on excess RE according to the generation profile, e-SAF's displacement of fossil usage is still more abatement-worthy than CCS with conventional jet fuel (Millinger et al., 2021).

7. Conclusions

Our modeling of the power sector transition over time illustrates the significant cost savings that e-SAF pathways can unlock if they are designed to operate flexibly. Critically, this could allow e-SAF pathways to become cost competitive with incumbent SAF pathways such as HEFA-SPK sooner than anticipated – provided countries deliver on their announced plans for the transformation of their power generation systems.

We drew several notable conclusions from this analysis:

1) There will be sufficient high-quality surplus renewable electricity to meet or exceed U.S. jet fuel demand in 2050 (up to 164% under certain conditions).
2) In the near- to mid-term, surplus renewable power could already support cost-effective production of high-integrity e-SAF in leading jurisdictions such as the Upper Mississippi, New England, and Northwest Power Pool -- even when fossil-based electricity is still part of the national grid mix. By drawing upon abundant wind generation and existing industrial ethanol fermentation CO_2, e-SAF synthesized in the Midwest alone could deliver a bulk of the 2030 national SAF Grand Challenge target of 3 billion gallons, at prices below $1000/tonne.
3) Power prices for the electrolysis operator in a supply-driven electric system can slash production costs by as much as half compared to baseline power prices in the current demand-driven rigid system. This makes e-SAF abatement costs the most competitive among SAF pathways.

4) The grid receives substantial benefits in terms of expediting the power sector's energy transition: curtailment is nearly eliminated with the introduction of any level of PtL flexibility; moreover, when the option of two-way electrolysis (and fuel cell reverse mode) is online, grid planners are able to retire fossil infrastructure earlier, as well as reliably deliver baseload demand on less installed generation, storage, and interregional transmission capacity compared to the reference non-PtL case. These savings are made possible by system efficiency gains per unit of infrastructure investment.

Therefore, high manufacturing costs of the present day ought to be viewed as a challenge to embrace, rather than as an immutable barrier. Not only is e-fuel adoption feasible – it also is necessary to attain global net zero goals across sectors.

The technological and market maturity of a multi-step process train is typically reported based on its lowest-TRL step. As such, the public discussion surrounding cost projections and market readiness often overlooks one or both of the following: (a) the high TRLs of other steps in the process train are obscured when reporting only the overall market readiness, and (b) opportunities for creative redesign, e.g. linking up with the power sector to provide DSM tools, which may in turn spur faster technological learning rates.

Our results also show that when SAF pathways are assessed based on abatement costs, e-SAF have a far more cost-efficient price per ton of CO_2 abated than other pathways. This is particularly noteworthy for a jurisdiction like Europe, where an EU ETS allowance price of €100/tCO_2 is a real possibility and would provide a sufficient incentive to cover the future abatement costs for e-SAFs, i.e., to fill up the price gap between e-SAFs and fossil jet fuel. Cap-and-trade systems, or other policy instruments delivering equivalent outcomes, should become the main driver for allocating resources to SAF pathways proportionately to the magnitude of their environmental attributes. But this will happen only if the EU ETS zero CO_2 combustion rating for biofuels and e-fuels is corrected and aligned with CORSIA's life-cycle approach -- one which grants emissions reductions benefits proportionally to the actual lifecycle emissions scores.

By providing key grid balancing services, e-SAF production can help reduce the cost of integrating renewable electricity and therefore the cost of the power sector's energy transition, while at the same time securing a lower cost of electricity for the e-SAF producer. Combination electrolyzer-fuel cells are not alone among flexible technologies with bi-directional capabilities for grid balancing. However, electrolyzer-fuel cells for PtL help decarbonize other sectors simultaneously and are a crucial linking carrier for renewable electrons. This opens an opportunity for countries with high generation potential to export renewable power in "portable" liquid form.

This study illustrates the tremendous potential for producing SAF with the highest environmental integrity and catalyzing grid transformation. Furthermore, the adoption of PtL technology serves not only aviation, but also other hard-to-decarbonize sectors with vested interests in production of long-chain synthetic hydrocarbons, such as maritime transport.

We reiterate that fully capitalizing on synergies is of paramount importance, both across sectors and within the e-SAF production pathway itself. The global decarbonization puzzle is too complex of a

challenge for each sector to address in isolation. The insights from our study reveal tangible avenues for combining problems to craft efficient, long-lasting solutions.

References

Adelung, S. (2022). Global sensitivity and uncertainty analysis of a Fischer-Tropsch based Power-to-Liquid process. *Journal of CO_2 Utilization, 65*(102171). doi:10.1016/j.jcou.2022.102171

Adelung, S., S. Maier & R.-U. Dietrich (2021). Impact of the reverse water-gas shift operating conditions on the Power-to-Liquid process efficiency. *Sustainable Energy Technologies and Assessments, 43*. doi:10.1016/j.seta.2020.100897

Becattini, V., P. Gabrielli & M. Mazzotti (2021). Role of Carbon Capture, Storage, and Utilization to Enable a Net-Zero-CO_2-Emissions Aviation Sector. Industrial & Engineering Chemistry Research 2021 60 (18), 6848-6862. doi: 10.1021/acs.iecr.0c05392.

Bekoe, K. (2023, October 5). Zero Petroleum's DirectFT technology.

Beuttler, C., L. Charles & J. Wurzbacher (2019). The Role of Direct Air Capture in Mitigation of Anthropogenic Greenhouse Gas Emissions. *Frontiers in Climate*. doi:10.3389/fclim.2019.00010

Breyer, C., M. Fasihi & A. Aghahosseini (2020). Carbon dioxide direct air capture for effective climate change mitigation based on renewable electricity: a new type of energy system sector coupling. *Mitigation and Adaptation Strategies for Global Change*(25), 43-65. doi:10.1007/s11027-019-9847-y

Breyer, C., M. Fasihi, C. Bajamundi & F. Creutzig (2019). Direct Air Capture of CO_2: A Key Technology for Ambitious Climate Change Mitigation. *Joule, 3*(9), 2053-2057. doi:10.1016/j.joule.2019.08.010

Chen, C., J. Khosrowabadi & S. Sheehan (2018). Progress toward Commercial Application of Electrochemical Carbon Dioxide Reduction. *Chem*, 2571-2586. doi:10.1016/j.chempr.2018.08.019

Cinti, G., A. Baldinelli, A. Di Michele & U. Desideri (2016). Integration of Solid Oxide Electrolyzer and Fischer-Tropsch: A sustainable pathway for synthetic fuel. *Applied Energy, 162*, 308-320. doi:10.1016/j.apenergy.2015.10.053

Dees, J., K. Oke, H. Goldstein, S.T. McCoy, D.L. Sanchez, A.J. Simon & W. Li (2023). Cost and Life Cycle Emissions of Ethanol Produced with an Oxyfuel Boiler and Carbon Capture and Storage. Environ Sci Technol. 2023 Apr 4;57(13):5391-5403. doi: 10.1021/acs.est.2c04784

Deutz, S., & A. Bardow (2021). Life-cycle assessment of an industrial direct air capture process based on temperature–vacuum swing adsorption. *Nature Energy*(6), 203–213. doi:https://doi.org/10.1038/s41560-020-00771-9

Dieterich, V., A. Buttler, A. Hanel, H. Spliethoff & S. Fendt (2020). Power-to-liquid via synthesis of methanol, DME or Fischer–Tropsch-fuels: a review. *Energy and Environmental Science, 13*(10), 3207-3252. doi: 10.1039/D0EE01187H

Dittrich, L., M. Nohl, E. Jaekel, S. Foit, L. Haart & R. Eichel (2019). High-Temperature Electrolysis: A Versatile Method to Sustainably Produce Tailored Syngas Compositions. *Journal of the Electrochemical Society, 166*(13), F871-75. doi: 10.1149/2.0581913jes

Esquivel-Elizondo, S., A. Hormaza Mejia, T. Sun, E. Shrestha, S.P. Hamburg, I.B. Ocko (2023). Wide range in estimates of hydrogen emissions from infrastructure. *Frontiers in Energy Research, 11*. doi: 10.3389/fenrg.2023.1207208

Fasihi, M., D. Bogdanov & C. Breyer (2016). Techno-Economic Assessment of Power-to-Liquids (PtL) Fuels Production and Global Trading Based on Hybrid PV-Wind Power Plants. *Energy Procedia, 99*, 243-268. doi: 10.1016/j.egypro.2016.10.115

Fasihi, M., O. Efimova & C. Breyer (2019). Techno-economic assessment of CO_2 direct air capture plants. *Journal of Cleaner Production, 224*, 957-980. doi: 10.1016/j.jclepro.2019.03.086

Grahn, M., E. Malmgren, A. Korberg, M. Taljegard, J.E. Anderson, S. Brynolf, ... & T.J. Wallington (2022). Review of electrofuel feasibility—cost and environmental impact. *Progress in Energy*. doi:10.1088/2516-1083/ac7937

Hauch, A., R.B.Kungas, A. Hansen, J. Hansen, B. Mathiesen & M. Mogensen (2020). Recent advances in solid oxide cell technology for electrolysis. *Science, 370*(6513). doi:10.1126/science.aba6118

Hoffman, A.L., A.R. Kemanian & C.E. Forest (2020). The response of maize, sorghum, and soybean yield to growing-phase climate revealed with machine learning. *Environmental Research Letters, 15*(094013). doi: 10.1088/1748-9326/ab7b22

International Civil Aviation Organisation (2021). CORSIA Default Life Cycle Emissions Values for CORSIA Eligible Fuels, 3rd Edition. Retrieved from https://www.icao.int/environmental-protection/CORSIA/Documents/ICAO%20document%2006%20-%20Default%20Life%20Cycle%20Emissions%20-%20November%202021.pdf

International Civil Aviation Organisation (2022). *SAF Rules of Thumb*. Retrieved from https://www.icao.int/environmental-protection/Pages/SAF_RULESOFTHUMB.aspx

International Energy Agency (2021a). *Net Zero by 2050: A Roadmap for the Global Energy Sector*. Retrieved from https://www.iea.org/reports/net-zero-by-2050

International Energy Agency (2021b). *Is carbon capture too expensive?* Retrieved from https://www.iea.org/commentaries/is-carbon-capture-too-expensive

London Science Museum (Compiler). Gantry from Mechanical Tree prototype. Retrieved from https://collection.sciencemuseumgroup.org.uk/objects/co8718404/gantry-from-mechanical-tree-prototype-designed-by-klaus-lackner-2017-gantries

International Renewable Energy Agency (2018). *Hydrogen from renewable power: Technology outlook for the energy transition*. Abu Dhabi: International Renewable Energy Agency. Retrieved from https://www.irena.org/-/media/files/irena/agency/publication/2018/sep/irena_hydrogen_from_renewable_power_2018.pdf

International Renewable Energy Agency (2019). *Innovation landscape brief: Renewable Power-to-Hydrogen*. Abu Dhabi: International Renewable Energy Agency. Retrieved from https://www.irena.org/-/media/Files/IRENA/Agency/Publication/2019/Sep/IRENA_Power-to-Hydrogen_Innovation_2019.pdf

International Renewable Energy Agency (2020). *Green Hydrogen Cost Reduction: Scaling up Electrolysers to Meet the 1.5ºC Climate Goal*. Abu Dhabi: International Renewable Energy

Agency. Retrieved from https://irena.org/-/media/Files/IRENA/Agency/Publication/2020/Dec/IRENA_Green_hydrogen_cost_2020.pdf

Keith, D., G. Holmes, D. St. Angelo & K. Heidel (2018). A Process for Capturing CO_2 from the Atmosphere. *Joule, 2*(8), 1573-1594. doi:10.1016/j.joule.2018.05.006

König, D. H., M. Freiberg, R.-U. Dietrich & A. Wörner (2015). Techno-economic study of the storage of fluctuating renewable energy in liquid hydrocarbons. *Fuel, 159*, 289-297. doi:10.1016/j.fuel.2015.06.085

Kuhl, K. (2021). *Electrochemical conversion of coal-derived CO_2 into fuels and chemicals using a modified PEM electrolyzer*. Opus 12. Retrieved from https://www.osti.gov/servlets/purl/1778958

Küngas, R. (2020). Electrochemical CO2 Reduction for CO Production: Comparison of Low- and High-Temperature Electrolysis Technologies. *Journal of the Electrochemical Society, 167*(4). doi:10.1149/1945-7111/ab7099

Lugovoy, O., S. Gao, J. Gao & K. Jiang (2021). Feasibility study of China's electric power sector transition to zero emissions by 2050. *Energy Economics, 96*. doi:/10.1016/j.eneco.2021.105176

Malins, C. (2017). *What role is there for electrofuel technologies in European transport's low carbon future?* Cerulogy. Retrieved from https://www.cerulogy.com/wp-content/uploads/2022/10/Cerulogy_What-role-electrofuels_November2017_v1_3.pdf

McQueen, N., K. Vaz Gomes, C. McCormick, K. Blumanthal, M. Pisciotta & J. Wilcox (2021). A review of direct air capture (DAC): scaling up commercial technologies and innovating for the future. *Progress in Energy, 3*. doi:10.1088/2516-1083/abf1ce

Millinger, M., P. Tafarte, M. Jordan, A. Hahn, K. Meisel & D. Thrän (2021). Electrofuels from excess renewable electricity at high variable renewable shares: cost, greenhouse gas abatement, carbon use and competition. *Sustainable Energy & Fuels, 5*, 828-843. doi:10.1039/d0se01067g

National Academies of Science, Engineering and Medicine (2019). *Negative Emissions Technologies and Reliable Sequestration: A Research Agenda*. Washington, DC: The National Academies Press. doi:10.17226/25259

Ocko, I.B. & S.P.Hamburg (2022). Climate consequences of hydrogen emissions. *Atmospheric Chemistry and Physics, 22, 9349–9368*. doi: 10.5194/acp-22-9349-2022.

Ozkan, M., S.P. Nayak, A. Ruiz & W. Jiang (2022). Current status and pillars of direct air capture technologies. *iScience, 25*(4). doi:10.1016/j.isci.2022.103990

Peterson, D., J. Vickers & D. DeSantis (2020a). Hydrogen Production Cost From High Temperature Electrolysis, U.S. Department of Energy's Hydrogen and Fuel Cells Program Record 20006. Retrieved from https://www.hydrogen.energy.gov/pdfs/20006-production-cost-high-temperature-electrolysis.pdf

Peterson, D., J. Vickers & D. DeSantis (2020b). Hydrogen Production Cost From PEM Electrolysis, U.S. Department of Energy's Hydrogen and Fuel Cells Program Record 19009. Retrieved from https://www.hydrogen.energy.gov/docs/hydrogenprogramlibraries/pdfs/19009_h2_production_cost_pem_electrolysis_2019.pdf

Pio, D.T., A.C.M. Vilas-Boas, V.D. Araújo, N.F.C. Rodrigues & A. Mendes (2023). Decarbonizing the aviation sector with Electro Sustainable Aviation Fuel (eSAF) from biogenic CO_2 captured at pulp mills. *Chemical Engineering Journal, 463*(142317). doi:10.1016/j.cej.2023.142317

Piris-Cabezas, P. (2022). *The High-Integrity Sustainable Aviation Fuels Handbook*. Environmental Defense Fund. Retrieved from https://www.edf.org/sites/default/files/2022-08/EDF%20HIGH-INTEGRITY%20SAF%20HANDBOOK.pdf

Platts Jet Fuel Price Monitor (2024). *S&P Global Commodity Insights*. Retrieved from https://www.spglobal.com/commodityinsights/en/oil/refined-products/jetfuel

PowerGenome Settings (n.d.). Retrieved from https://github.com/PowerGenome/PowerGenome/wiki/Settings-files#demand

Rojas-Michaga, M., S. Michailos, E. Cardozo, M. Akram, K. Hughes, D. Ingham & M. Pourkashanian (2023). Sustainable aviation fuel (SAF) production through power-to-liquid (PtL): A combined techno-economic and life cycle assessment. *Energy Conversion and Management, 292*(117427). doi:10.1016/j.enconman.2023.117427

Sabatino, F., A. Grimm, F. Gallucci, M. van Sint Annaland, G. Jan Kramer & M. Gazzani (2021). A comparative energy and costs assessment and optimization for direct air capture technologies. *Joule, 5*, 2047-2076. doi:10.1016/j.joule.2021.05.023

Sadiq, M., M. Batten, X. Mulet, C. Freeman, K. Konstas, J. Mardel, J. Tanner, D. Ng, X. Wang, S. Howard, M. Hill, A. Thornton (2020). A Pilot-Scale Demonstration of Mobile Direct Air Capture using Metal-Organic Frameworks. *Advanced Sustainable Systems, 4*. doi:10.1002/adsu.202000101

Schivley, G. E. (2024). PowerGenome v0.6.1. Zenodo. doi:10.5281/zenodo.8329515

Schmidt, O., A. Gambhir, I. Staffell, A. Hawkes, J. Nelson & S. Few (2017). Future cost and performance of water electrolysis: An expert elicitation study. *International Journal of Hydrogen Energy, 42*(52), 30470-30492. doi:doi.org/10.1016/j.ijhydene.2017.10.045

Schmidt, P., W. Weindork, A. Roth, V. Batteiger & F. Riegel (2016). *Power-to-Liquids, Potentials and Perspectives for the Future Supply of Renewable Aviation Fuel*. Dessau-Roßlau: Ludwig-Bölkow-Systemtechnik GmbH; Bauhaus Luftfahrt e.V. Umweltbundesamt.

Seymour, K., M. Held, B. Stolz, G. Georges & K. Boulouchos (2024). Future costs of power-to-liquid sustainable aviation fuels produced from hybrid solar PV-wind plants in Europe. *Sustainable Energy Fuels, 8*, 811-825. doi:10.1039/D3SE00978E

Sheehan, S., M. Garedew & C. Chen (2022). Single-Step Production of Alcohols and paraffins from CO_2 and H_2O at Metric Ton Scale. *ACS Energy Letters, 7*, 988-992. doi:10.1021/acsenergylett.2c00214

Sherwin, E. D. (2021). Electrofuel synthesis from Variable Renewable Electricity: An Optimization-Based Techno-Economic Analysis. *Environmental Science & Technology, 55*, 7583-7594. doi:10.1021/acs.est.0c07955

Stauffer, N. (2020, July). A new approach to carbon capture: Researchers design an effective treatment for both exhaust and ambient air. *Energy Futures*(Spring 2020). Retrieved from https://news.mit.edu/2020/new-approach-to-carbon-capture-0709

Sun, T., E. Shrestha, S.P. Hamburg, R. Kupers & I.B. Ocko (2024). Climate Impacts of Hydrogen and Methane Emissions Can Considerably Reduce the Climate Benefits across Key Hydrogen Use Cases and Time Scales. *Environmental Science & Technology, 58 (12), 5299-5309.* doi:10.1021/acs.est.3c09030

Terwel, R., & J. Kerkhoven (2018). *Carbon Neutral Aviation with Current Engine Technology: The take-off of synthetic kerosene production in the Netherlands.* Kalavasta B.V. Retrieved from https://kalavasta.com/assets/reports/Kalavasta_Carbon_Neutral_Aviation.pdf

Treyer, K., R. Sacchi & C. Bauer (2022). *Life Cycle Assessment of synthetic hydrocarbons for use as jet fuel: "Power-to-Liquid" and "Sun-to-Liquid" processes.* Paul Scherrer Institut, Laboratory for Energy System Analysis, Villigen. Retrieved from https://www.psi.ch/en/ta/projects/synfuels-psi-empa-joint-initiative

United States Departments of Energy, Transportation & Agriculture (2021, September). Memorandum of Understanding: SAF Grand Challenge. Retrieved from https://www.energy.gov/sites/default/files/2021-09/S1-Signed-SAF-MOU-9-08-21_0.pdf

United States Energy Information Administration (EIA) (2023). U.S. Fuel Ethanol Plant Production Capacity. Retrieved from https://www.eia.gov/petroleum/ethanolcapacity/

United States Department of Agriculture (USDA) (2024). Grain Crushings and Co-Products Production Monthly Report: June 2024. Retrieved from https://downloads.usda.library.cornell.edu/usda-esmis/files/n583xt96p/c247gj19b/8910mj73x/cagc0824.pdf

United States Federal Aviation Administration (FAA) (2021). United States National Aviation Climate Action Plan. Retrieved from https://www.faa.gov/sites/faa.gov/files/2021-11/Aviation_Climate_Action_Plan.pdf

Wentrup, J., G.R. Pesch, & J. Thoming (2022). Dynamic operation of Fischer-Tropsch reactors for power-to-liquid concepts: A review. *Renewable and Sustainable Energy Reviews, 162.* doi:10.1016/j.rser.2022.112454

World Economic Forum (2020). *Clean Skies for Tomorrow: Sustainable Aviation Fuels as a Pathway to Net-Zero Aviation. Insight Report.* WEF and McKinsey & Company. Retrieved from https://www3.weforum.org/docs/WEF_Clean_Skies_Tomorrow_SAF_Analytics_2020.pdf

Young, J., N. McQueen, C. Charalambous, S. Foteinis, O. Hawrot, M. Ojeda, H. Pilorgé, J. Andresen, P. Psarras, P. Renforth, S. Garcia & M. van der Spek (2023). The cost of direct air capture and storage can be reduced via strategic deployment but is unlikely to fall below stated cost targets. *One Earth, 6*(7), 899-917. doi:10.1016/j.oneear.2023.06.004